

NGU Report 98.008

Gravity modelling and petrophysical data from  
western Norway

Report no.: 98.008		ISSN 0800-3416	Grading: Open
Title: Gravity modelling and petrophysical data from western Norway			
Authors: J.R. Skilbrei & O. Kihle		Client: Statoil, Mobil Exploration, Phillips Petroleum	
County: Sogn og Fjordane		Commune:	
Map-sheet name (M=1:250.000) Florø		Map-sheet no. and -name (M=1:50.000)	
Deposit name and grid-reference:		Number of pages: 36	Price (NOK): 125
		Map enclosures:	
Fieldwork carried out: 1995-1997	Date of report: 13.02.98	Project no.: 2671.00	Person responsible: <i>Jørn S. Røed</i>
Summary:			
<p>Gravity data have been interpreted with a view to determining the depth extent of the Devonian Hornelen Basin. We find that the Hornelen Basin has a maximum depth of 3-4 km (below sea level). Uncertainty in the modelling originates in the low density contrast between the Devonian sedimentary rocks and the crystalline basement rocks. There is a rather close correlation between surface geology and gravity maps, which provides constraints on the gravity modelling.</p> <p>Summary statistics of petrophysical property data are reported. The magnetic susceptibility data show that, on a regional scale, most magnetic anomaly sources will be felsic gneisses and metavolcanic Caledonian rocks. The low Q-values indicate the dominance of induced magnetization in these rocks.</p>			
Keywords: Magnetometri	Petrofysikk	Geofysikk	
Berggrunnsgeologi			
		Fagrapport	

## LIST OF CONTENTS

1. INTRODUCTION.....	4
2. APPLIED DENSITY DATA .....	4
3. BRIEF DESCRIPTION OF POTENTIAL FIELDS.....	5
4. REGIONAL-RESIDUAL SEPARATION OF GRAVITY .....	6
5. GRAVITY MODELS.....	6
6. PHYSICAL PROPERTIES OF ROCKS .....	7
6.1 Density data.....	11
6.2 Magnetic property data .....	11
7. DISCUSSION .....	12
8. CONCLUSIONS.....	13
9. ACKNOWLEDGEMENTS .....	14
10. REFERENCES.....	14

## LIST OF FIGURES

Fig. 1	Simplified geological map of the Sunnfjord area (modified mainly from Osmundsen & Andersen, 1994).
Fig. 2a	Bouguer anomaly map
Fig. 2b	Residual gravity map
Fig. 3	Aeromagnetic map
Figures 4-6	Gravity models
Figures 7-19	Histograms of density and magnetic susceptibility
Fig. 20	Plot of magnetic susceptibility versus density. Units in SI.
Fig. 21	Plot of magnetic susceptibility versus Q-value. Unit in SI.

## **1. INTRODUCTION**

The reported work is part of the project named ‘Onshore-offshore tectonic links in Western Norway - An integrated approach’. It is a collaboration project between Statoil, Mobil Exploration, NFR, Phillips Petroleum, NPD, NGU and the University of Oslo. This report focuses on the interpretation of the onshore gravity data that we have acquired from the study area, and on the petrophysical data. The main objective was to model the thickness of the Devonian basin, and to provide summary statistics for the petrophysical property data (density, magnetic susceptibility and intensity of magnetic remanence). An interpretation of onshore and offshore magnetic and gravity fields is reported by Smethurst (1998).

Before this project started, only a few gravity stations existed from the Devonian basins and the basement in western Norway. In order to model the thickness of the sedimentary basins, a better gravimetric coverage was needed. To supplement NGU’s database, gravity measurements were made along roads in 1995. New gravity measurements that cover the coastal zone were made in 1996 which enabled us to tie the separate gravity surveys over land and shelf. In 1996 and 1997, supplementary gravity measurements were made onshore, with helicopter transportation. This was important because many of the roads run more or less along the dominating geological strike. In Fig. 2a, the Bouguer anomaly map is shown together with the positions of the gravity stations. For the marine areas, we have used a slightly smoothed 3 km by 3 km gravity grid which was provided by NPD (processed by Amarok Niasa).

## **2. APPLIED DENSITY DATA**

Gravity modelling is dependent on the applied density contrast and the interpreted magnitude of the residual anomaly. These parameters must therefore be considered carefully. The petrophysical properties of representative rock samples are reported below (Table 1 and figures 7-21). We obtained a mean density of 2747 kg/m<sup>3</sup> for 473 samples of gneiss (granitic to monzodioritic composition, hornblende gneiss, banded gneiss, mica gneiss) of the Western Gneiss Region (WGR) which was used in the gravity model. Only 1% of the volume of the WGR is assumed to be occupied by eclogites in this calculation. Depending on the number of amphibolites and eclogites included in the specimens, the calculated mean value will be higher in value than if the gneisses contain only insignificant volumes of these rocks.

270 samples of metasedimentary and metavolcanic Caledonian rocks gave a mean density of 2753 kg/m<sup>3</sup> (Table 1). A mean density of 2723 kg/m<sup>3</sup> was calculated from 96 samples of Devonian sedimentary rocks.

The density of 2747 kg/m<sup>3</sup> which has been assigned to the gneisses of the WGR is probably reasonable, because felsic gneisses predominate with subordinate amounts of amphibolites and negligible volumes of eclogites, and because of the comparatively large number of samples. However, one problem is to estimate how common the basic hypabyssal bodies are.

### **3. BRIEF DESCRIPTION OF POTENTIAL FIELDS**

The Bouguer anomalies over the study area are shown in Fig. 2a. There is a strong regional west to east negative gradient that reflects primarily an eastwards increase in Moho depths (e.g., Dyrelius 1985, Elming 1988, Skilbrei 1988a). This effect is removed in the residual gravity map shown in Fig. 2b. The gravity fields are displayed together with the main geological boundaries on land, and with main faults offshore (from the NPD). The strongest gradients in the gravity fields occur along Sognefjorden and Nordfjorden. These water bodies are included in the gravity models (see below). Just to the west of the coastline, a coastparallel gravity high occurs following the onlapping sequence of sediments.

On land, gravity lows are located above the Hornelen Basin (Fig. 2b). The gravity lows and the gravity contours show a correspondence in area and outline with the Hornelen Basin. In addition, gravity lows are associated with some of the granitic gneisses within the WGR. Also, the heterogeneous basement causes many local gravity highs from the WGR, primarily above basic and mafic rock units. This is for example well expressed to the west of Førde (Fig. 2b).

The aeromagnetic map is shown in Fig. 3. The area and the scale correspond to that of the gravity maps (Figs. 2a & 2b). The aeromagnetism is discussed in more detail by Smethurst (1998). There is a regional aeromagnetic low above the Hornelen Basin. The lowest values occur above the western and northwestern parts of the basin. This coincides closely with the pattern seen on the residual gravity map (Fig. 2b). The gneisses southeast of the Hornelen Basin appear to be non-magnetic. Even with this in mind, we interpret the presence of a small amplitude, local positive aeromagnetic high, that occurs just east of the central part of the basin, to be caused by shallow crystalline basement underneath the sediments in this part of the basin. This strengthens the inference made from the residual gravity map that the Hornelen Basin is deepest in the northwestern part (see later).

#### **4. REGIONAL-RESIDUAL SEPARATION OF GRAVITY**

The amplitude of the negative residual anomaly will partly determine the thickness of the sedimentary bodies in the model calculation. We have applied a regional field that was manually chosen (graphically fitted) during the modelling, choosing the residual to be zero where the density is close to that of the reference crust. The reference crust has a density of 2747 kg/m<sup>3</sup> which is the basis for calculating the density contrast between the Devonian sedimentary rocks and the crystalline basement. For qualitative interpretations, a high-pass version of the Bouguer gravity is shown in Fig. 2b.

Because of the ambiguity of gravity modelling, we present both maximum and minimum depth extent models. The minimum thickness model is based on combining a minimum density contrast (mean value minus ½ standard deviation) with a maximum amplitude of the residual gravity values. The maximum density contrast (mean value plus ½ standard deviation) combined with a minimum residual amplitude is applied providing a minimum depth. Finally, our preferred model is presented. This model is based on the mean density contrast and a reasonable regional-residual analysis.

To avoid using a residual anomaly of maximum amplitude we have chosen a regional field which takes into account the granitic gneisses that occur both on the north side and the south side of the Hornelen Basin. A small negative anomaly is thus defined north and south of the Hornelen Basin, where light granitic rocks occur.

#### **5. GRAVITY MODELS**

The meaning of Bouguer anomalies in this area of uneven topography must be considered carefully. The Bouguer gravity field on the map is not the same as the field which would have been observed at the datum (sea level), because the amplitude and shape of anomalies are partly due to remaining density differences appropriate to the elevation of measurements. We have tested the following: 1) Considered the Bouguer anomalies at constant density (2670 kg/m<sup>3</sup>) with the top of the bodies at the datum. 2) Interpreted the data taking into account geological bodies from the ground surface downwards using 2 1/2 D models. The terrain correction was carried out using a digital terrain model on a 100m by 100m grid. Errors due to the differences between constant (2670 kg/m<sup>3</sup>) and actual densities of geological units are in the Bouguer anomalies. These errors are reduced when the bodies extend to the ground surface. Residual errors are attributed to the approximated modelling of the topographic surface and errors in density and simplified geological model. We found that the difference

between the models using sea-level as the top of the model bodies (Figs. 4 & 5), and the models where the topography makes up the top of the models (Fig. 6), is small. This negligible difference is due to the small difference in density used in the reduction of the gravity data (Bouguer plate correction and terrain corrections) and the density of the major rock units.

Gravity models along the south to north running profile A-A' are shown in Fig. 4. In Fig. 4a, the most realistic model is shown, and Fig. 4b depicts the deepest possible model. Density contrasts of 45 and 30 ( $\text{kg/m}^3$ ) have been used for the models in a and b; respectively. An east to west running profile is shown in Fig. 5 (profile B-B'), representing our preferred model.

Profile C-C' runs NW-SE (see Fig. 6). In this latter profile, we have incorporated Caledonian metavolcanic rocks, mangerites, hornblende gneiss, banded gneiss, granitic gneiss, as well as Devonian sedimentary rocks. In Fig. 6c, we have included a rather thick sequence of Devonian conglomerates (with a density of  $2737 \text{ kg/m}^3$ ). This is reasonable, because conglomerates occur close to the basin flanks, and because the Håsteinen Basin, which represents the erosional remnant of the bottom part of a Devonian basin, consists primarily of breccias and conglomerates.

From the modelling work we conclude that the likely depth extent of the Hornelen Basin is around 3-4 km. The other Devonian basins in Nordvestlandet are thin, as deduced also from the geological maps (e.g. Sigmond et al., 1984).

## **6. PHYSICAL PROPERTIES OF ROCKS**

The aim of this study is to illustrate the rock physical properties of the main lithologies in Nordvestlandet, and to determine the density contrast between the sedimentary rocks and the basement. Results from a total of 2504 rock samples now exist in our data base from the study area. Many of these specimens are eclogites. Therefore, during the present project, 940 new rock samples representing main lithologies have been collected and measured with respect to the physical properties density, magnetic susceptibility and remanent magnetization intensity. The density is determined as a wet bulk density with an accuracy of  $10 \text{ kg/m}^3$ . Magnetic susceptibility is measured using the natural frequency method with a relative error of about 1% (Skilbrei, 1988b) and a resolution of 0.0001 SI.

**Table 1. Petrophysical properties of rocks and rock-units; a, b, and c denote total sample, low-magnetic fraction and high magnetic fraction, respectively. Units are in SI. The standard deviations of susceptibility and intensity of remanence are in decades. Susceptibility and intensity of remanence have logarithmic mean values.**

Rock unit/ type	No.	Density				Intensity of remanence					Susceptibility					
		Min	max	mean	std	No.	min	max	log-mean	std	No	min	max	log-mean	std	
<b>PRECAMBRIAN BASEMENT, WESTERN GNEISS REGION</b> Gneiss	a	473	2555	3354	2747	126	416	2.636	7453.70	26.88	0.73	699	0.00002	9.43000	0.00168	0.72886
	b											462			0.00061	0.36889
	c											237			0.01215	0.43127
Granitic gneiss	a	31	2606	3272	2692	122	27	2.716	7453.70	50.07	1.07	31	0.00005	0.40688	0.00545	0.79432
	b											11			0.00085	0.49777
	c											20			0.01513	0.53564
Grandioritic gneiss	a	15	2645	3206	2779	166	14	3.10	3049.10	29.78	0.88	15	0.00019	0.29892	0.00340	0.91981
	b											9			0.00076	0.35228
	c											6			0.03243	0.57618
Micagneiss	a	48	2632	3040	2744	81	44	3.13	1163.22	24.88	0.61	48	0.00012	0.09991	0.00171	0.71644
	b											32			0.00064	0.40523
	c											16			0.01200	0.36958
Hornblendegneiss	a	13	2682	2808	2758	36	13	4.65	48.02	16.23	0.26	19	0.00035	0.01092	0.00114	0.46255
	b											15			0.00071	0.25241
	c											4			0.00671	0.15240
Augen gneiss	a	47	2622	2969	2704	73	45	2.63	2870.19	36.11	0.75	47	0.00007	0.07485	0.00432	0.82187
	b											18			0.00055	0.49785
	c											29			0.01553	0.36616
Felsic plutonic rocks	a	21	2580	2737	2654	36	15	4.46	185.32	27.80	0.54	21	0.00017	0.02845	0.00606	0.64675
	b											4			0.00039	0.33974
	c											17			0.01160	0.27037
Intermed. plutonic rocks	a	7	2632	2671	2656	15	1	56.74	56.74	56.74	0.00	7	0.00007	0.02769	0.00549	0.81633
	b											1			0.00007	0.00000
	c											6			0.01135	0.28255
Mafic plutonic rocks	a	6	2721	3424	3160	254	1	5.75	5.75	5.75	0.00	6	0.00032	0.00143	0.00061	0.19546



Rock unit/ type	No.	Density				Intensity of remanence					Susceptibility					
		Min	max	mean	std	No.	min	max	log-mean	std	No	min	max	log-mean	std	
															0.00061	0.19546
<b>CALEDONIAN ROCKS</b>																
Felsic plutonic-, interm. plutonic-, mafic plutonic rocks, conglomerate, psammitic and pelitic rocks, basic volcanites, interm. volcanites, acid volcanites, greenschist, gneiss	a b c	270	2589	3089	2753	109	225	0.03	153.17	0.74	0.59	270 239 31	0.00001	0.22047	0.00043 0.00028 0.01187	0.69852 0.47244 0.44049
Gneiss	a b c	100	2604	2995	2722	71	76	0.08	153.17	0.70	0.55	100 87 13	0.00002	0.03428	0.00039 0.00024 0.00941	0.67255 0.41831 0.33802
Granitic-, granodioritic-, tonalitic gneiss, micagneiss	a b c	21	2611	2816	2716	62	15	0.08	153.17	1.30	0.74	21 20 1	0.00003	0.03428	0.00024 0.00019 0.03428	0.63451 0.42419 0.00000
Greenschist	a b c	27	2583	3066	2808	142	26	0.03	7.14	0.45	0.47	27 20 7	0.00024	0.07008	0.00110 0.00051 0.00974	0.66131 0.29127 0.48178
Greenschist, amphibolite, eclogite, hornblendeschist	a b c	17	2703	3066	2878	127	16	0.03	7.14	0.39	0.52	17 13 4	0.00024	0.07008	0.00115 0.00056 0.01181	0.64616 0.25116 0.48451
Conglomerate, psammitic- and pelitic rocks	a b c	111	2589	3017	2732	83	95	0.03	45.38	0.77	0.64	111 100 11	0.00001	0.03607	0.00038 0.00026 0.01175	0.69745 0.50536 0.32413

Rock unit/ type	No.	Density				Intensity of remanence					Susceptibility					
		Min	max	mean	std	No.	min	max	log-mean	std	No	min	max	log-mean	std	
<b>DEVONIAN</b>																
Conglomerate, psammitic- and pelitic rocks	a	96	2526	2833	2723	42	80	0.09	2.16	0.36	0.28	96	0.00015	0.01265	0.00053	0.40398
	b											90			0.00045	0.29305
	c											6			0.00673	0.15271
Conglomerate	a	14	2628	2833	2738	64	12	0.14	1.00	0.33	0.27	14	0.00017	0.01265	0.00153	0.61905
	b											8			0.00050	0.32810
	c											6			0.00673	0.15271
Psammitic and pelitic rocks	a	82	2526	2799	2721	36	68	0.09	2.16	0.36	0.28	82	0.00015	0.00216	0.00044	0.28895
	b											82			0.00044	0.28895

Table 1 presents summary statistics for the main rock units from the Precambrian and Caledonian rocks, as well as the Devonian sedimentary rocks. Figures 7-19 present frequency histograms of Caledonian, Precambrian and Devonian rocks (density and magnetic susceptibility data). The right tail in the histogram shown in Fig. 7 represents measurements on eclogites. These have been excluded from the calculation of mean values listed in Table 1.

## 6.1 Density data

The basement rocks in this region generally have a low to medium density, but high-density amphibolites, gabbros, eclogites and ultramafic rocks occur locally (see Table 1). The lithologies of the Caledonian allochthon show a wide range in density. The psammitic rocks and the basic rocks have the lowest and the highest densities, respectively. The mean density for the crystalline Caledonian rocks is  $2753 \text{ kg/m}^3$ , when ultramafic rocks have been excluded from the calculations. The mean density of Precambrian rocks of the Western Gneiss Region (WGR) is  $2747 \text{ kg/m}^3$ , when only 1% of the area is assumed to be occupied by eclogites. The density of the Devonian rocks is  $2723 \text{ kg/m}^3$ , which provides a relatively small density contrast between the Devonian basins and the basement that can be used in the gravity modelling.

## 6.2 Magnetic property data

The magnetic susceptibility producing aeromagnetic anomalies in basement areas is proportional to the magnetite content (e.g. Henkel, 1976). A plot of density versus magnetic susceptibility for main lithologies is shown in Fig. 20, in which each sample is represented by one symbol. The gneissic rocks from the WGR show a wide range of susceptibility values, and some of the felsic gneisses as well as the mafic rocks are moderately to strongly magnetised. The latter represent small volumes. Therefore, the felsic gneisses of acidic to intermediate composition are the likely sources of regional aeromagnetic anomalies from the Precambrian basement. These rocks plot in the upper left part of the diagram (Fig. 20).

The Caledonian rocks of the WGR generally show low magnetic susceptibility values. This includes most samples, except for some samples of greenstones, and gneisses of acidic to intermediate composition. In the density versus magnetic susceptibility diagram (Fig. 20), granitic and granodioritic rocks occur to the left in the diagram. The metasedimentary rocks as

well as the metavolcanites show a wide spread in density, while mafic rocks occur in the centre-right part of the diagram.

We inspect the Q-values (ratio of remanent to induced magnetization) from bivariate diagrams of susceptibility and Q-values (Fig. 21). The Q-values are around 0.4 for most rock types, and for those samples with susceptibility values above 0.01 SI, the mean Q-value is around 0.13 (see the plot of Q-value versus susceptibility in Fig. 21). Thus, for aeromagnetic measurements, one can assume that the magnetization is parallel to the Earth's magnetic field which simplifies the interpretation of most of the magnetic anomalies. An exception will be for some of the basic and mafic rock units.

## 7. DISCUSSION

1. The magnetic property data show that, on a regional scale, most magnetic anomalies are associated with felsic gneisses and metavolcanic Caledonian rocks. The low Q-values allow one to assume purely induced magnetization of these rocks. Basic rocks, including eclogites and amphibolites, as well as intermediate plutonic rocks, may give rise to local aeromagnetic anomalies. We interpret the magnetic susceptibility data of representative samples to indicate that on the shelf adjacent to this part of Western Norway, the most likely sources of the regional aeromagnetic anomalies are acidic to intermediate felsic gneisses and plutonic rocks. In addition, highly magnetised gabbroic massifs/high-grade basic rock complexes, like the Bergen Arcs and the Jotunheimen Massif, may exist in one or two places offshore Western Norway and Central Norway (Skilbrei 1989a, 1989b, Smethurst 1998); thus giving rise to large-amplitude aeromagnetic anomalies. Caledonian greenstone units may give rise to local anomalies offshore Nordvestlandet.

2. The basement rocks from the coastal areas of the WGR are more dense than basement rocks from eastern parts of Norway, e.g. to the east of the Sogn-Jotunheimen areas (Skilbrei 1988a, 1989b). This may be a general feature of Norway; along the coastal zone, which was close to the Caledonian subduction zone between Baltica and Laurentia, and subsequently was uplifted, the basement has different petrophysical properties, due to a higher metamorphic grade and a different metamorphic history. Differences in the original composition of the rocks may also be important.

3. A regional-residual gravity separation is always questionable and subjective. Where geological data and density data are available to evaluate and check properties of residual values, the manual subjective methods give the 'best' residual values both for qualitative and

quantitative interpretations of broad regional to smaller scale structures (e.g. Gupta and Ramani 1980, Fastland and Skilbrei 1989, Skilbrei 1988c, 1989c, Skilbrei and Sindre, 1991).

4. There is probably an upwarp in the Moho surface underneath the coastal region which is due to the Permo-Triassic rifting events. (The Mesozoic rifting and crustal thinning was located further west). This is interesting, because earlier gravity models (Skilbrei 1989b, 1989c) predict that there is also a minor upwarp in the Moho surface underneath the Bergen Arcs which trends northeasterly beneath the Hardangerfjorden area. This Moho-upwarp may trend further northeast, and/or exist underneath the Jotun Nappe Complex (Skilbrei 1989b, 1989c). It can be speculated that there is a continuous trend of decreased Moho-depths associated with the Faltungsgraben from the Hardangerfjorden area to Jotunheimen, perhaps representing Permo-Triassic rifting.

5. The modelling has been based on the following observations: (1) The gravity and magnetic fields correspond to outcropping lithologies, (2) The margins of the Hornelen Basin dip inwards. These assumptions are all reasonably well proven by published geological data and the new density data. The gravity models could be changed somewhat because the gravity effect is not particularly sensitive to changes in the deeper parts of models, and in addition, no gravity interpretation is unique (Dobrin 1960).

6. Although the negative gravity effects of the water makes interpretations difficult close to fjords (Skilbrei 1991), it is likely that the thickest part of the Hornelen Basin is in the west and the northwest (close to Bremangerlandet). Both the gravity values and the aeromagnetics, suggest that the basin is thinner in the eastern half than in the western part. Basement highs may exist locally within the eastern part of the basin where local gravity highs occur.

## **8. CONCLUSIONS**

There is a rather close correlation between geological maps and gravimetric and petrophysical data, which provide constraints on the number of possible gravity models. We suggest that the Hornelen Basin is 3-4 km thick, and the thickest part of the basin is in the northwestern and western margins of the basin.

The magnetic property data from the Sunnfjord area show that, on a regional scale, most magnetic anomalies will be due to felsic gneisses and metavolcanic Caledonian rocks. The low Q-values allows one to assume primarily induced magnetization of these rocks.

## 9. ACKNOWLEDGEMENTS

We thank O. Olesen, M. Smethurst and J.S. Rønning for valuable comments to the manuscript. T. Torsvik helped with the layout of figures 4-6.

## 10. REFERENCES

- Dobrin, M.B., 1960: Introduction to geophysical prospecting, 2nd edition. McGraw-Hill Pub, New York, Co., 446 pp.
- Dyrelius, D., 1985: A geophysical perspective of the Scandinavian Caledonides. *In*: D.G. Gee and B.A. Sturt (editors), The Caledonide Orogen-Scandinavia and Related Areas. John Wiley & Sons, Chichester: 185-194.
- Elming, S.A., 1988: Geological modelling based on gravity data from the central part of the Swedish Caledonides. *Geol. För. i Stockh. Forh.*, 110: 317-327.
- Fasteland, F., og Skilbrei, J.R. 1989: Tolkning av helikoptergeofysikk, gravimetri og petrofysikk innenfor kartblad 1723 III Steikjer, Nord-Trøndelag. *NGU Rapport 89.158*, 31 pp.
- Gupta, V.K. and Ramani, N., 1980: Some aspect of regional-residual separation of gravity anomalies in a Precambrian terrain. *Geophysics*, 45: 1422-1426.
- Henkel, H., 1976: Study of density and magnetic properties of rocks from Northern Sweden. *PAGEOPH*, 114/2, 23-32.
- Hurich, C.A., Palm, H., Dyrelius, D. and Kristoffersen, Y., 1989: Deformation of the Baltic continental crust during Caledonide intracontinental subduction: Views from seismic reflection data. *Geology*, 17: 423-425.
- Osmundsen, P.T. & Andersen, T.B. 1994: Caledonian compressional and late-orogenic extensional deformation in the Staveneset area, Sunnfjord, western Norway. *Journal of Structural Geology*, 16: 1385-1401.

- Sigmond, E.M.O, Gustavson, M. and Roberts, D., 1984: Bedrock Map of Norway. Scale 1: 1000,000. *Nor. geol. unders.* Trondheim.
- Skilbrei, J.R., 1988a: Geophysical interpretation of the Fosen-Namsos Western Gneiss Region and northern part of the Trondheim Region Caledonides, Central Norway. *Nor. geol. unders. Special Publ.*, 3: 70-79.
- Skilbrei, J.R. 1988b: Målenøyaktighet og reproduserbarhet ved måling av petrofysiske egenskaper i laboratorium og i felt; med forslag til endringer og utskifting av instrumenter. *NGU Rapport 88.001*, 25pp.
- Skilbrei, J.R. 1988c: Gravimetrikart for Trøndelag (M 1:500 000) og området fra 62 N til 67 N (M 1:1 mill.); med vurdering av metoder for regional-residual separasjon og kvalitativ tolkning av residualkart. *NGU-Rapport 88.003*, 18 pp.
- Skilbrei, J.R. 1989a: Petrofysiske undersøkelser, midt-Norge. *NGU-rapport 89.164*, 112pp.
- Skilbrei, J.R. 1989b: Structure of the Jotun Nappe Complex, southern Norwegian Caledonides: Ambiguity of gravity modelling and reinterpretation. *NGU-Report 89.169*, 27 pp.
- Skilbrei, J.R. 1989c: Geophysical expression of the Lærdal-Gjende Fault, Jotun Nappe Complex, southern Norwegian Caledonides. Abstract, *IAGA Bulletin No53, Part B*, pp. 120.
- Skilbrei, J.R. 1991: Om effekten av fjordene på tyngdekartene. *Intern NGU-Rapport 91.022*, 16 pp.
- Skilbrei, J.R. og Sindre, A. 1991: Tolkning av gravimetri langs ILP-profilet, Hemne-Storlien. *NGU-Rapport 91.271*. 27 pp.
- Skilbrei, J.R., Skyseth, T., and Olesen, O., 1991: Petrophysical Data and Opaque Mineralogy of High Grade and Retrogressed Lithologies: Implications for the Interpretation of Aeromagnetic Anomalies in Northern Vestranden, Central Norway Tectonophysics. In: P. Wasilewski and P. Hood (editors): Magnetic anomalies-Land and Sea. *Tectonophysics*, 192: 21-31.
- Smethurst, M., 1998: Onshore-Offshore tectonic links in western Norway: An interpretation of magnetic and gravity fields. Volume 1 and 2. *NGU Report 98.006*, 81 pp.



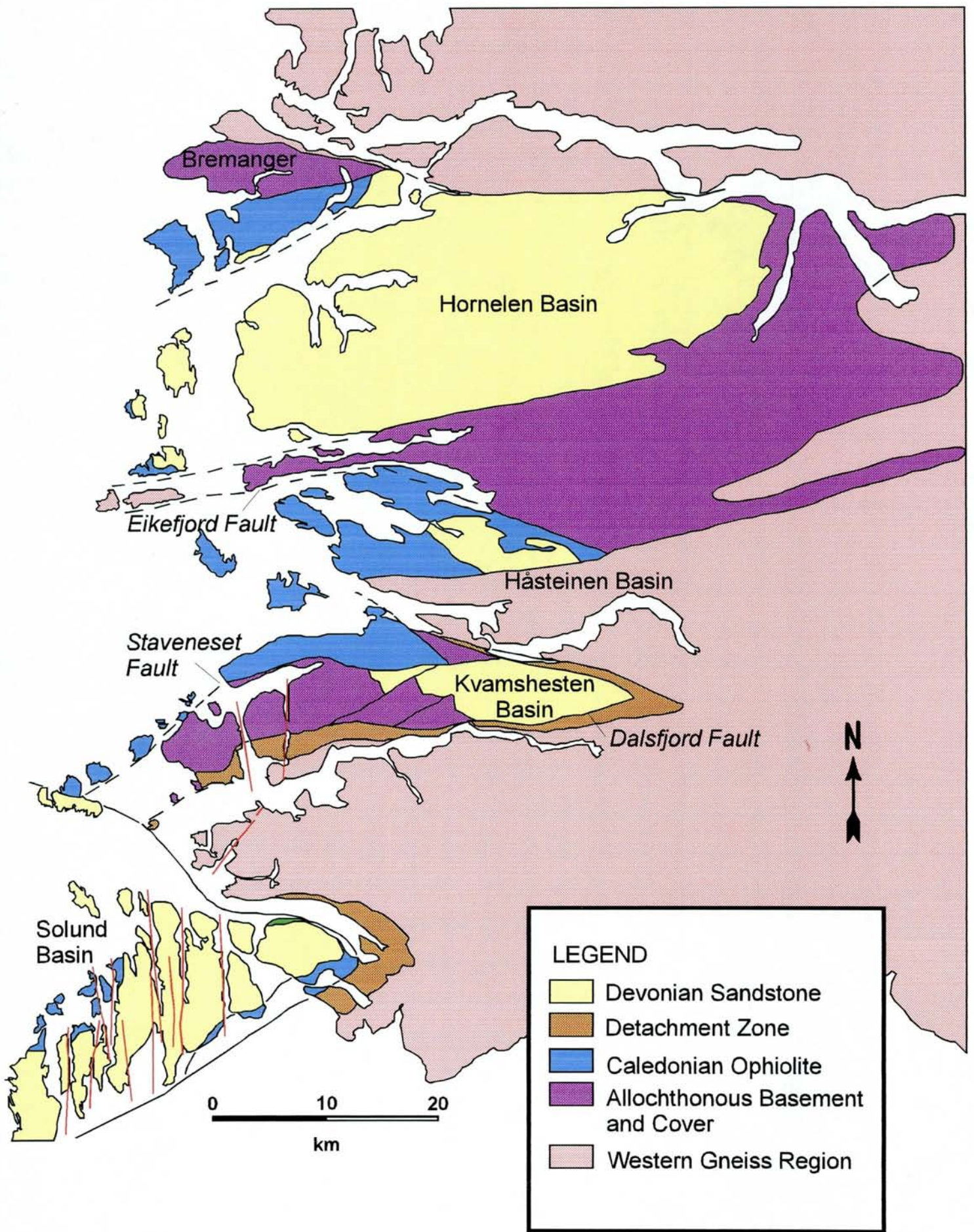


Fig. 1 Simplified geological map of the Sunnfjord area (from Osmundsen and Andersen, 1994)



# BOUGUER ANOMALIES

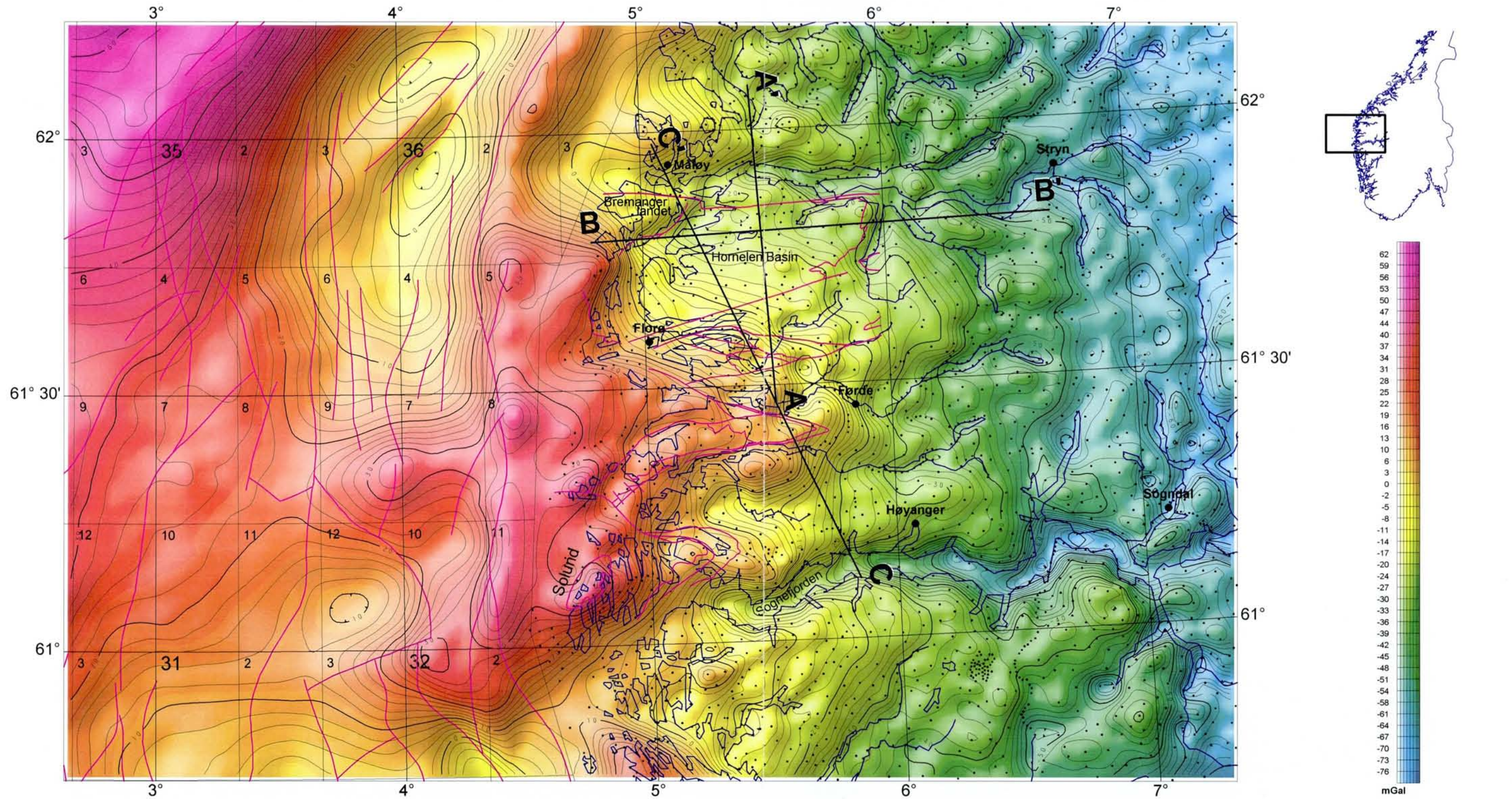


Figure 2a. Bouguer anomalies. Contour interval is 2 mGal. Profiles AA', BB' and CC' refer to gravity models shown in figures 4-6.

## Legend

- Gravity stations on land.
- Offshore faults (from NPD) and selected principal geological boundaries on land

10 0 10 20 30  
(kilometers)



## RESIDUAL GRAVITY ANOMALIES

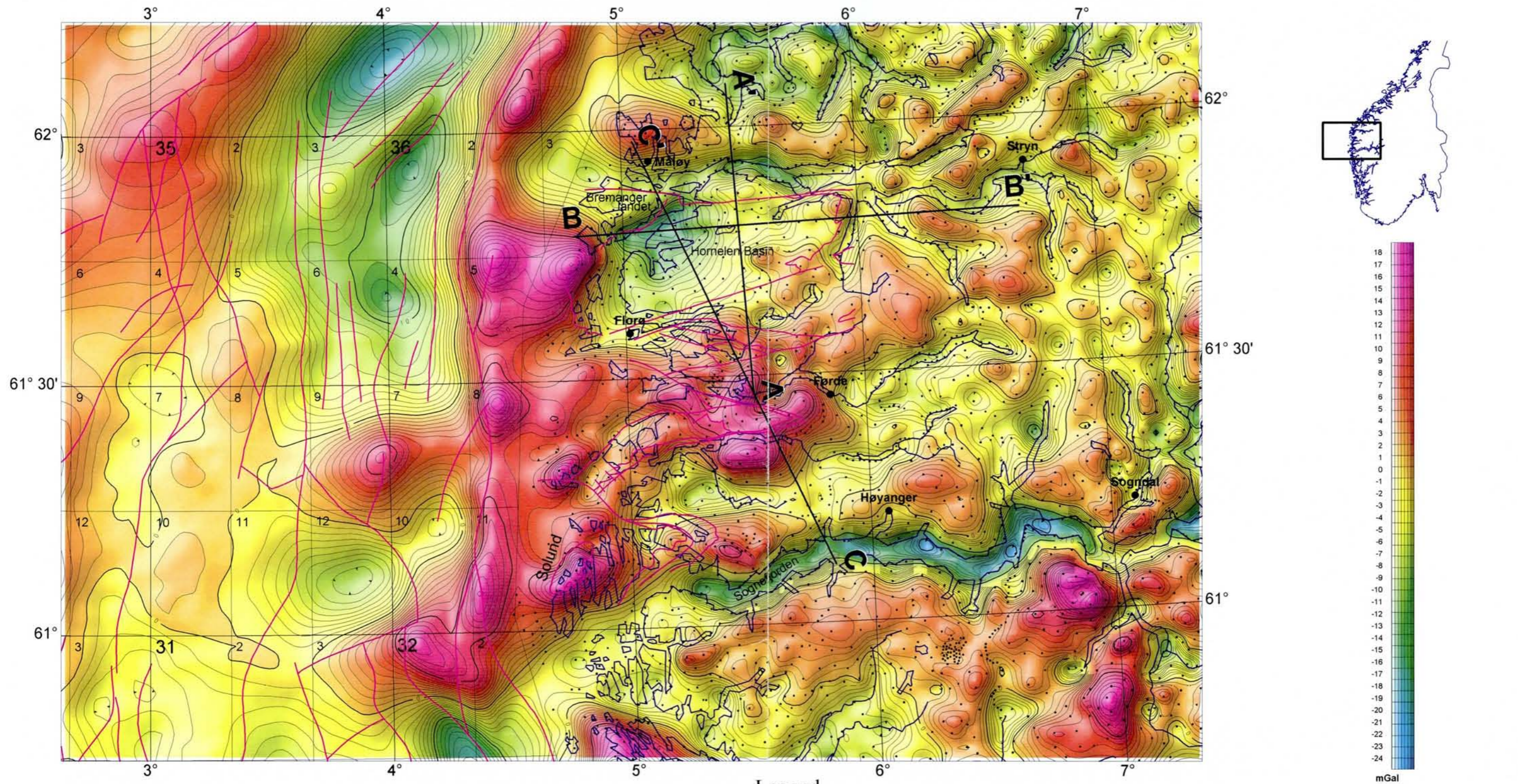


Figure 2b. Residual gravity anomalies. High pass filtered Bouguer anomalies with a cutoff wavelength of 120 km. Contour interval is 1 mGal. Profiles AA', BB' and CC' refer to gravity models shown in figures 4-6.

### Legend

- Gravity stations on land.
- Offshore faults (from NPD) and selected principal geological boundaries on land

10    0    10    20    30  
(kilometers)



# AEROMAGNETIC MAP

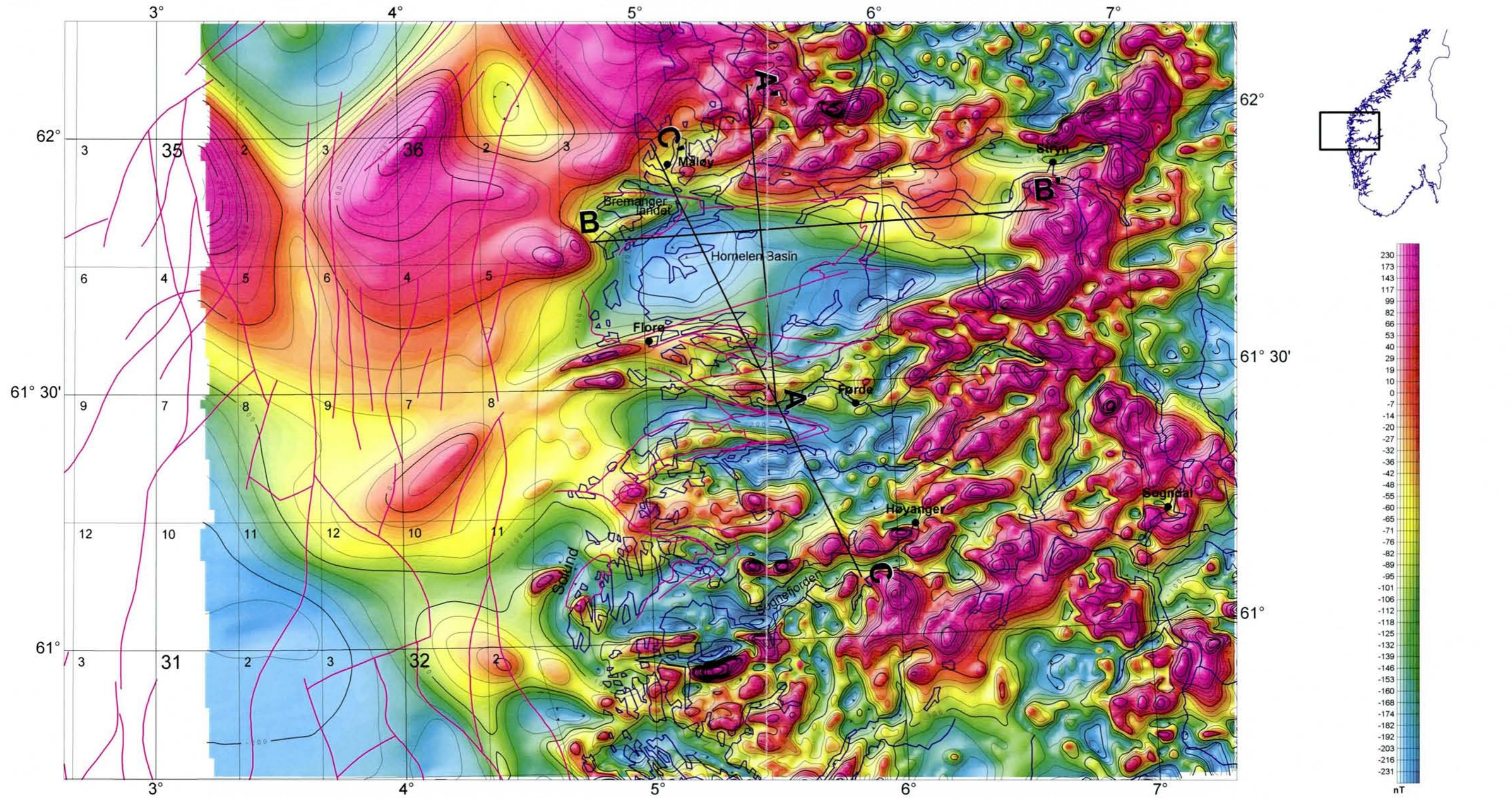


Figure 3. Aeromagnetic map. Total field anomalies. Contour interval is 25 nT. Profiles AA', BB' and CC' refer to gravity models shown in figures 4-6.

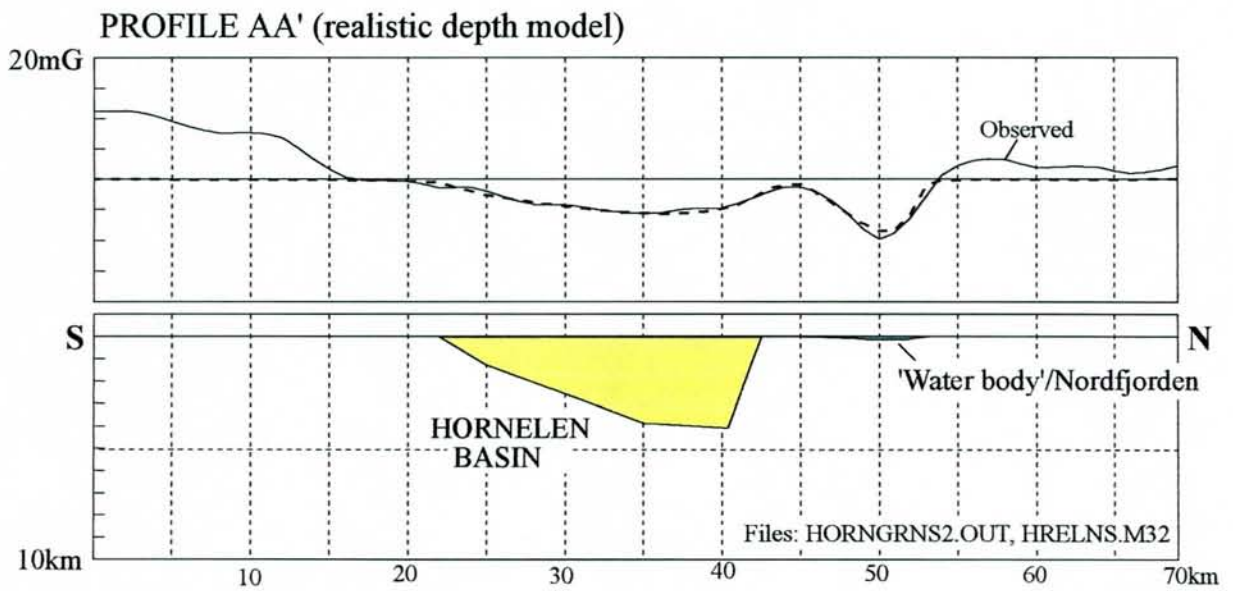
## Legend

- Offshore faults (from NPD) and selected principal geological boundaries on land

10 0 10 20 30  
(kilometers)



a)



b)

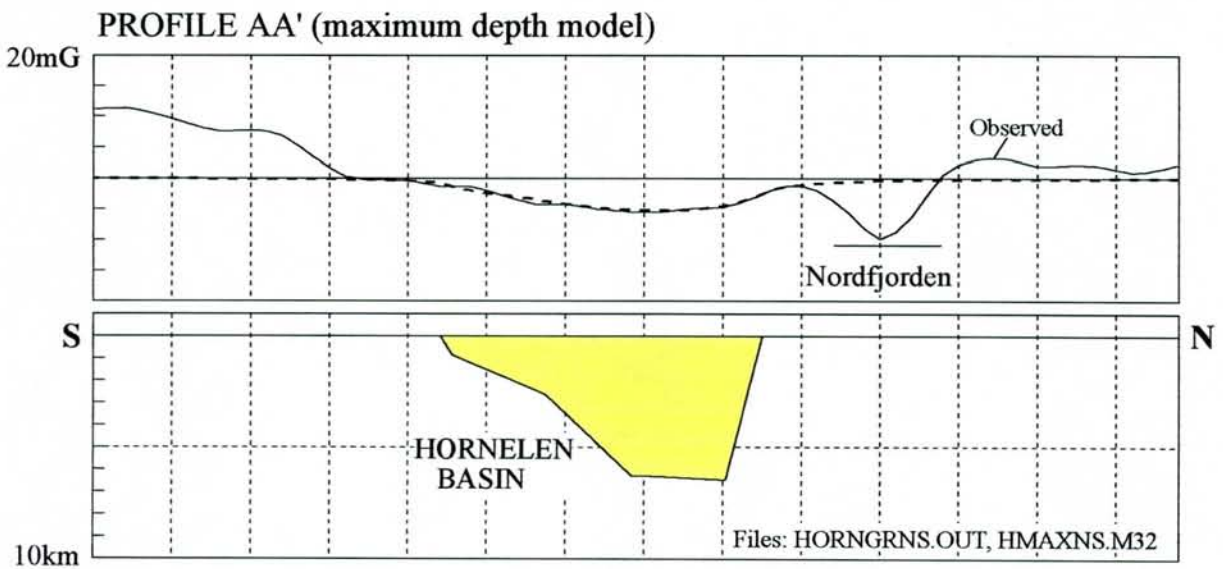
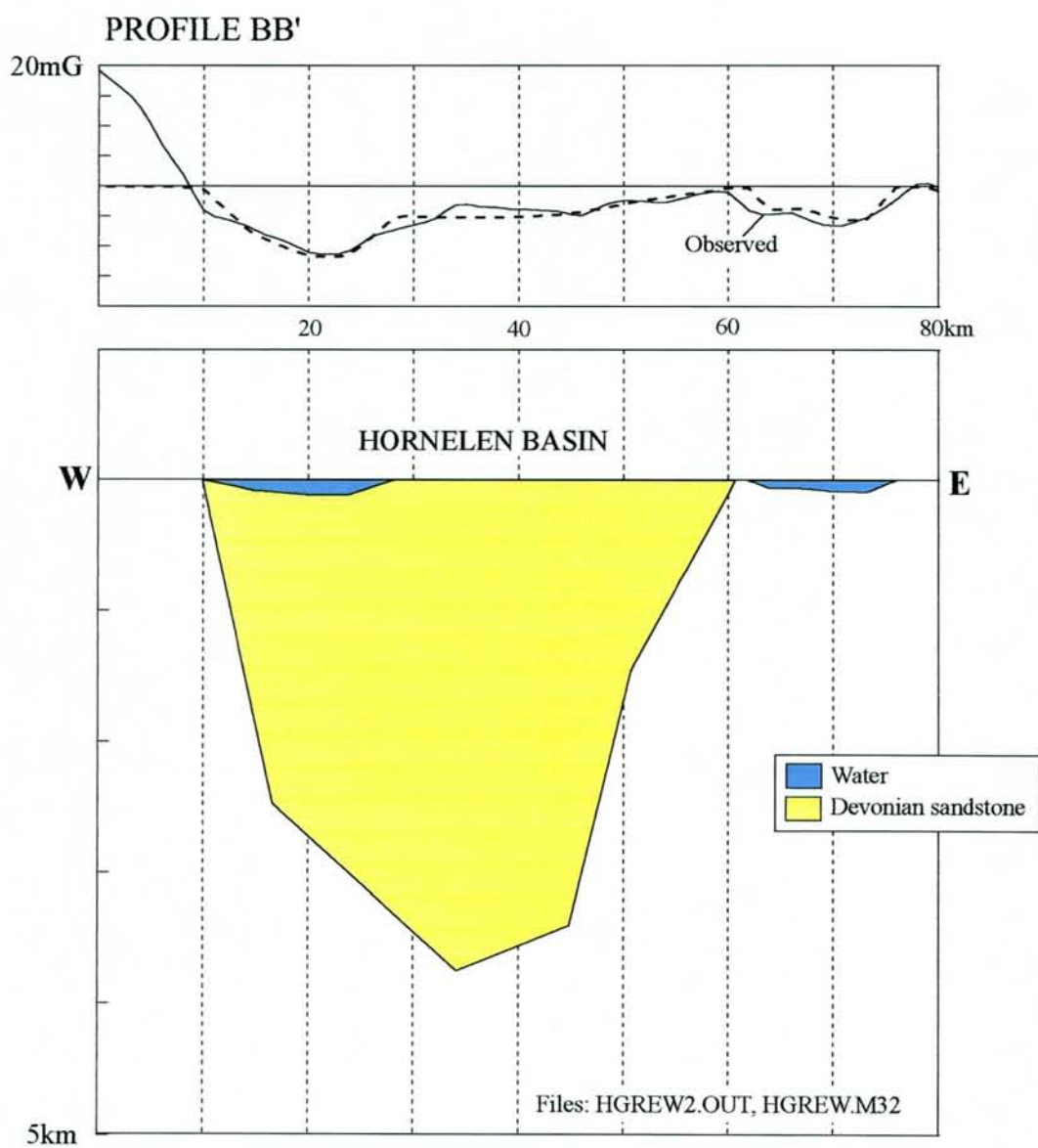
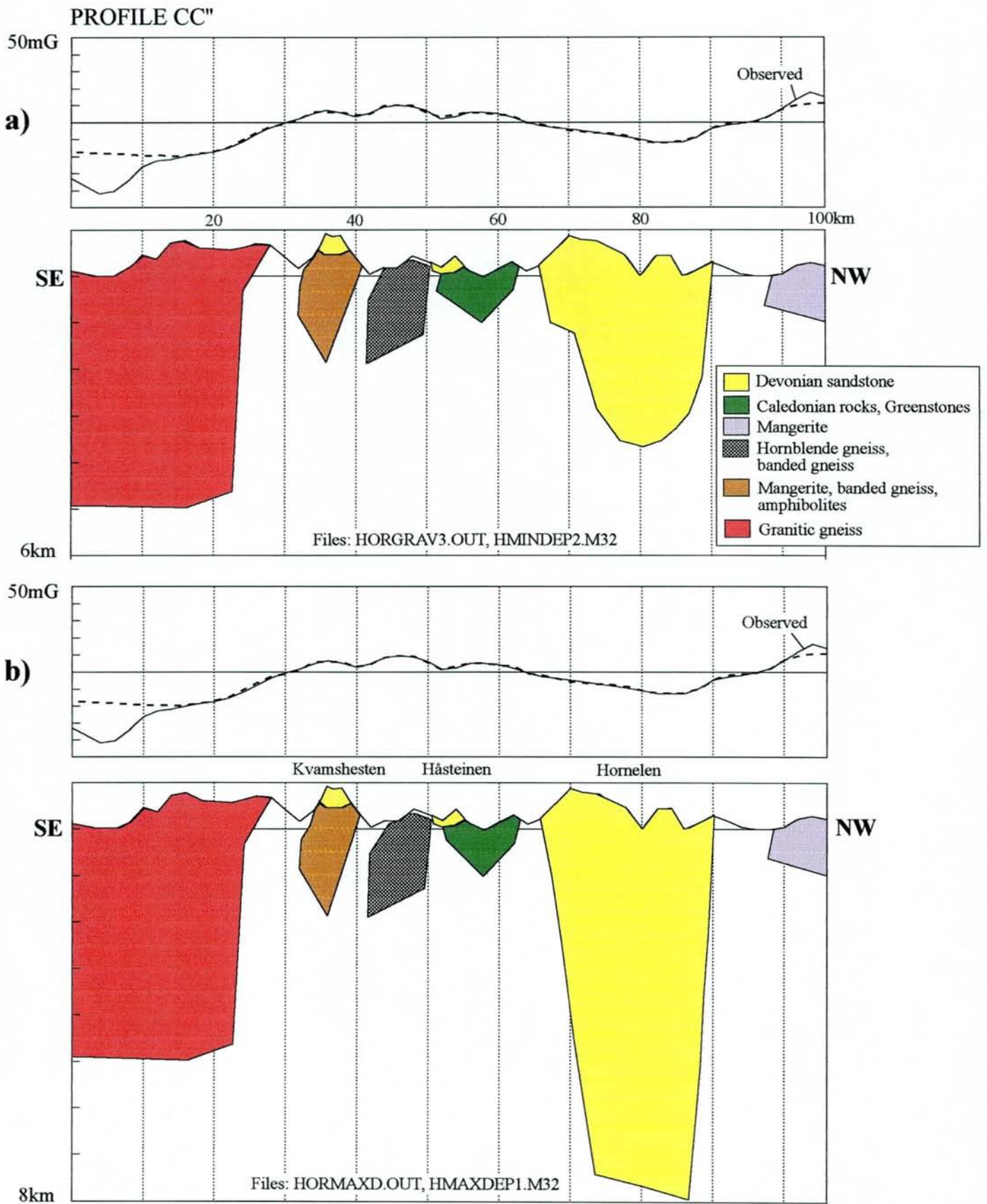


Figure 4  
Gravity model across the Hornelen Devonian Basin showing a 'realistic' (a) and a 'maximum' depth model (b). See Fig. 2 for location of profile.



**Figure 5**  
 Gravity model along east-west profile across the Hornelen Devonian Basin. See Fig. 2 for location of profile and text for further explanation.



**Figure 6**  
Gravity model along a NW-SE profile across the Sunnfjord area. See Fig. 2 for location of profile and text for further explanation.

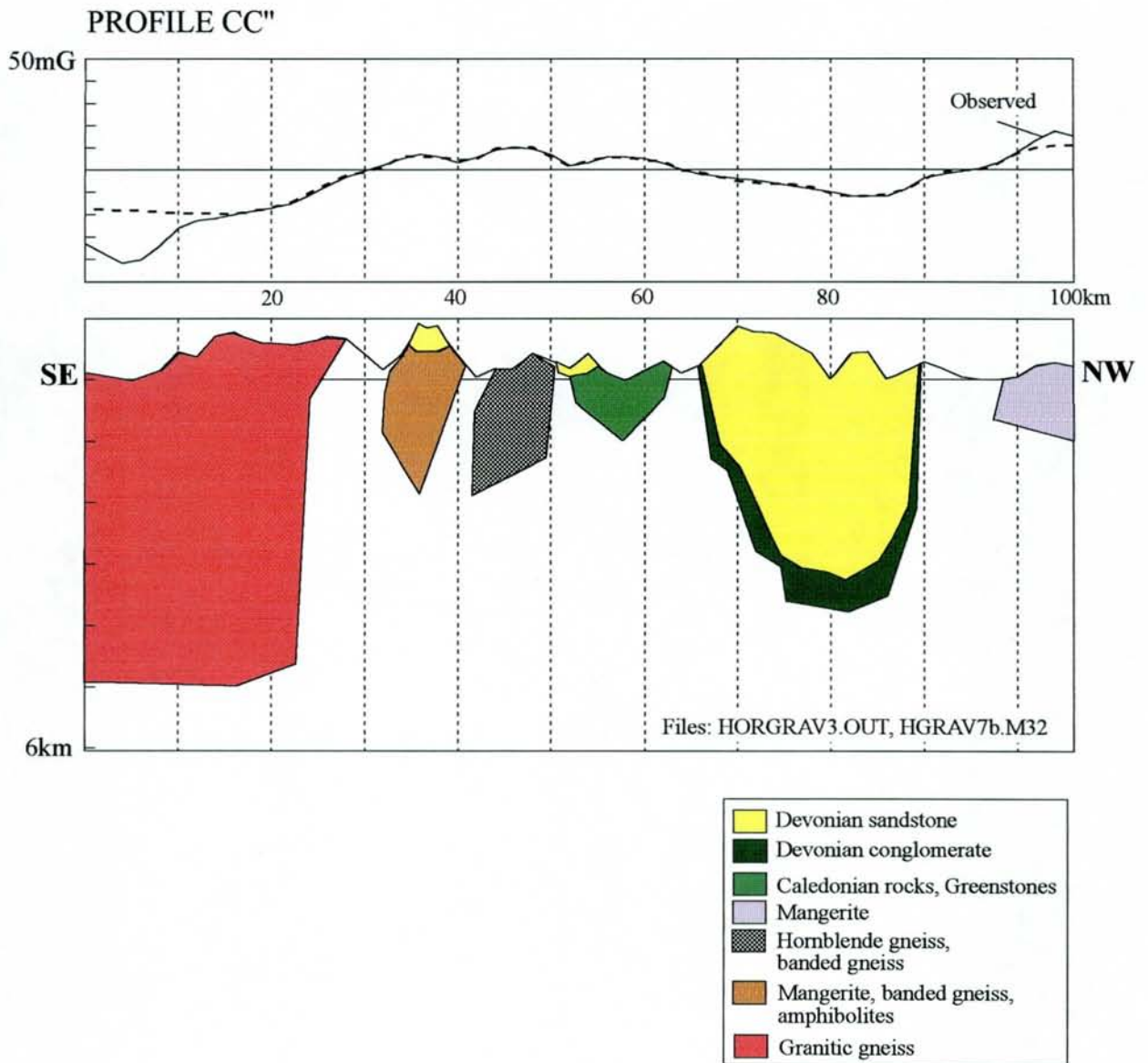
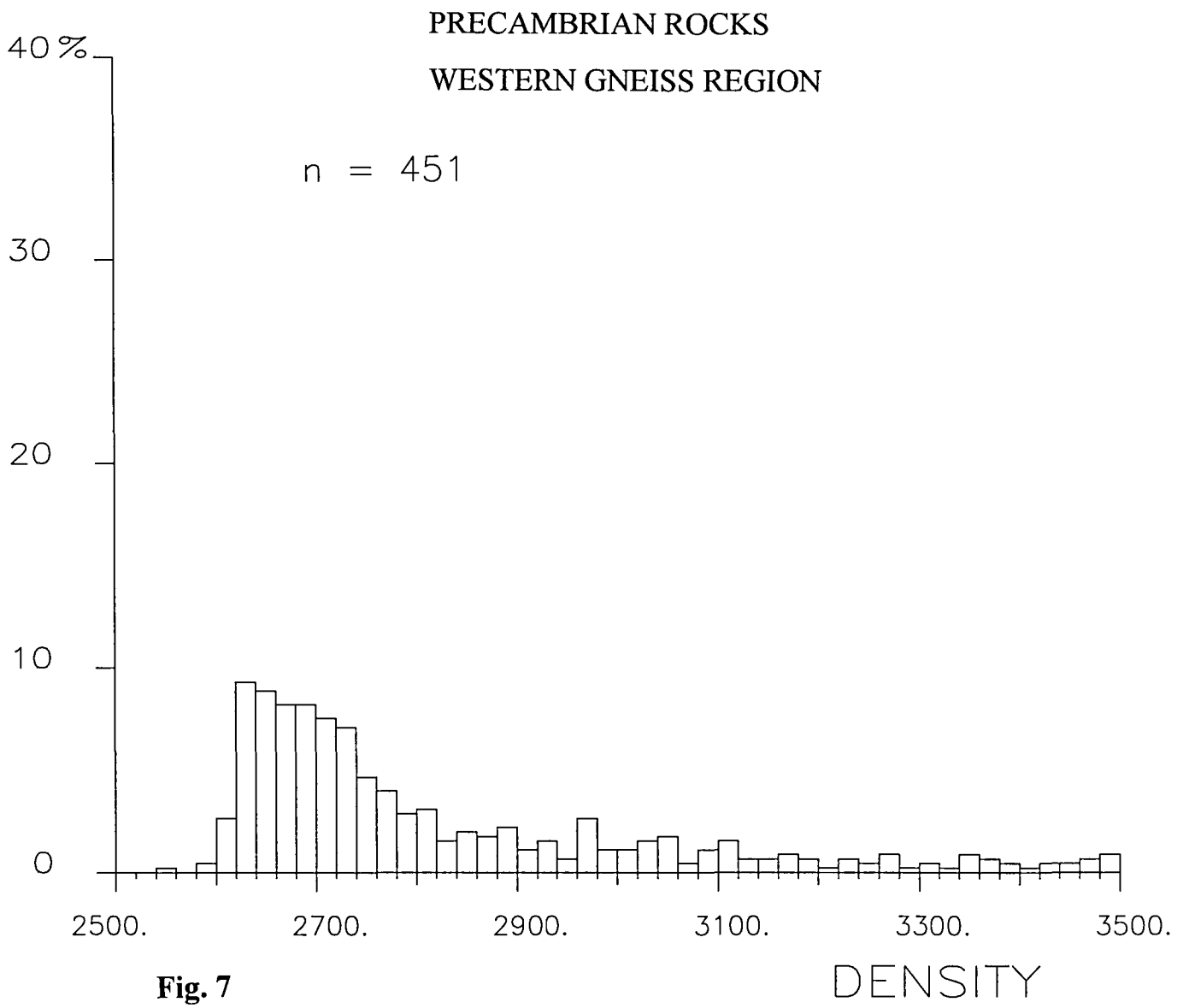


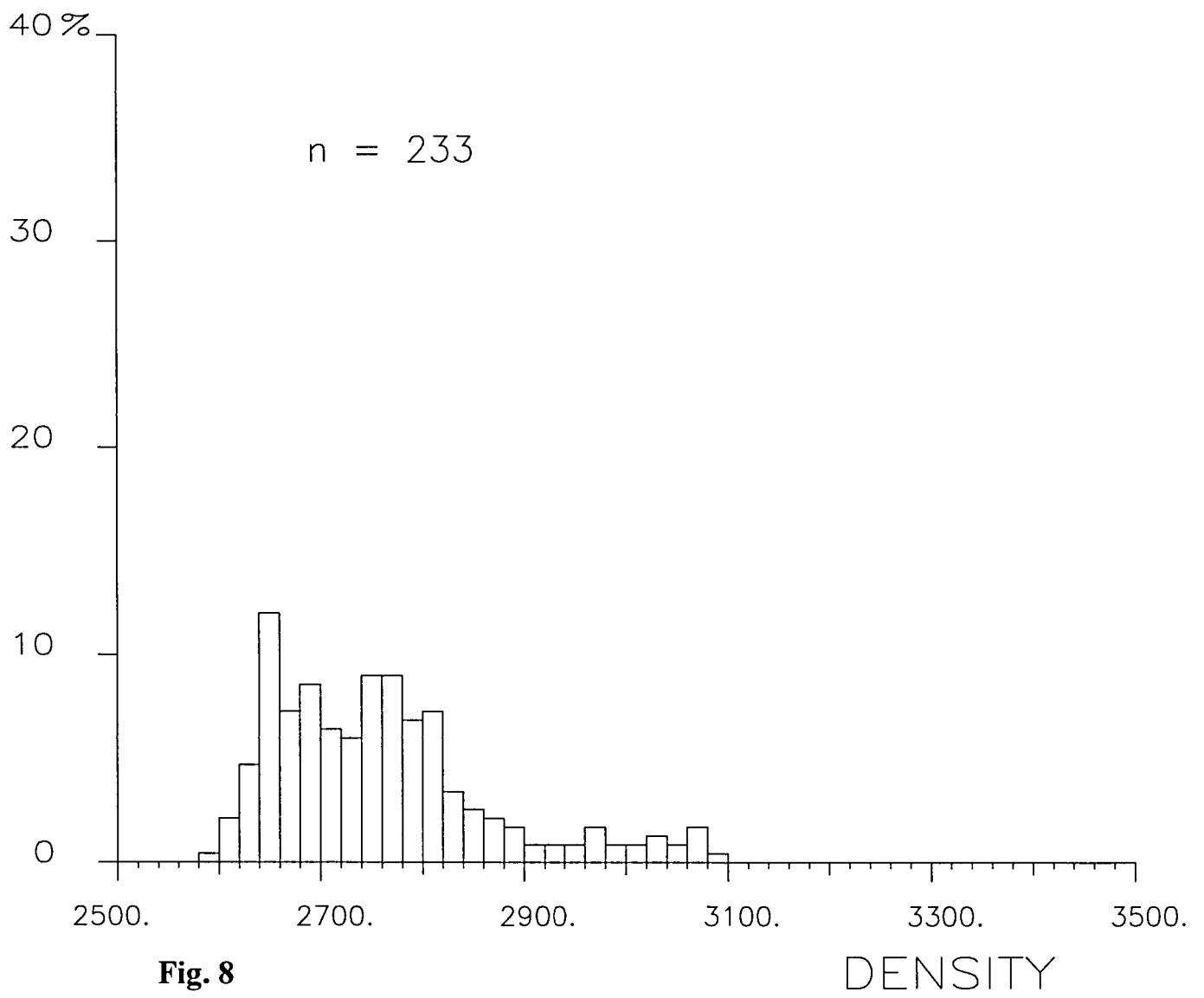
Figure 6c  
Gravity model along a NW-SE profile across the Sunnfjord area. See Fig. 2 for location of profile and text for further explanation.



**Fig. 7**



# CALEDONIAN ROCKS



# DEVONIAN SEDIMENTARY ROCKS

Conglomerate, psammitic rocks, pelitic rocks

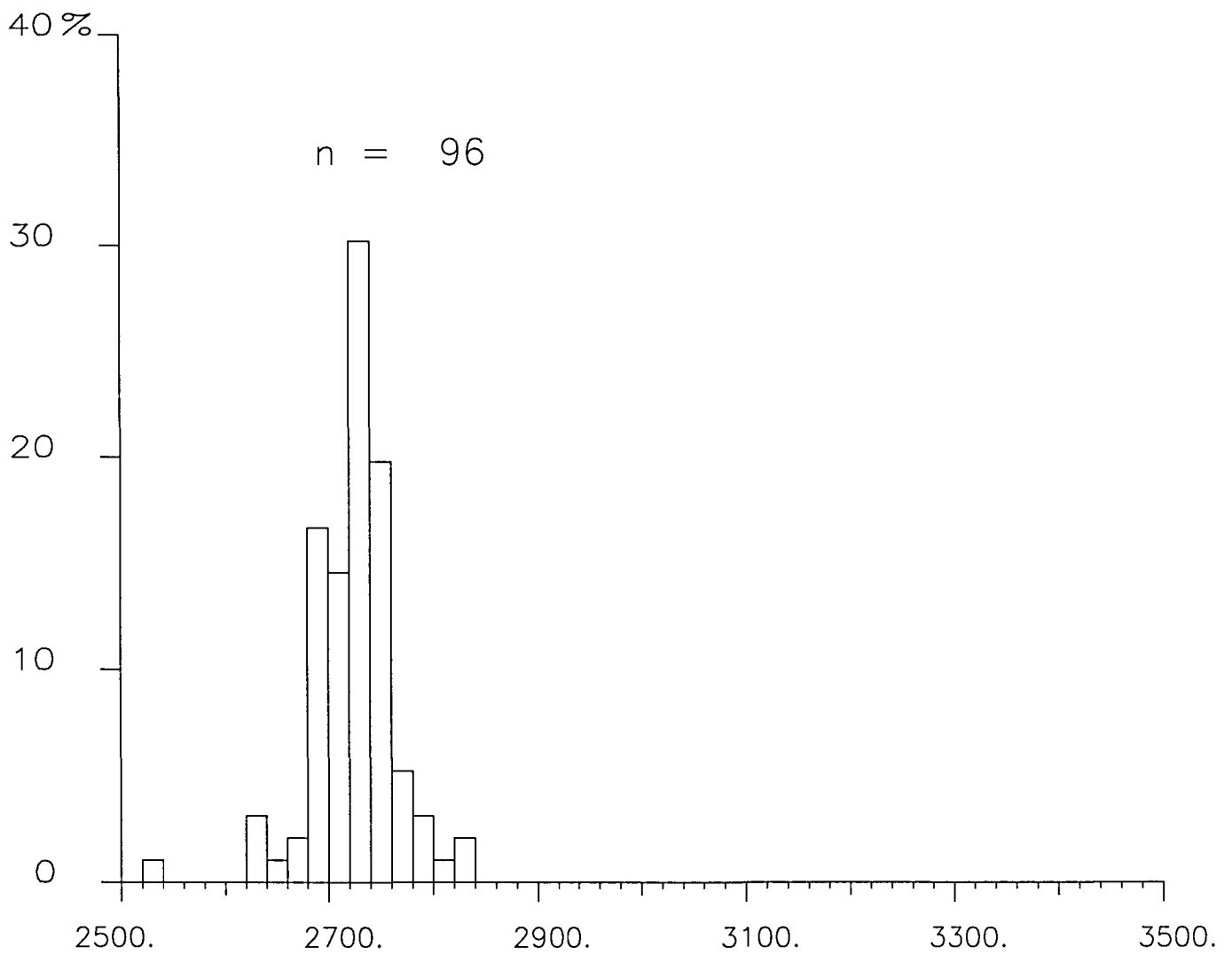


**Fig. 9**

DENSITY

PRECAMBRIAN ROCKS  
WESTERN GNEISS REGION  
Gneiss

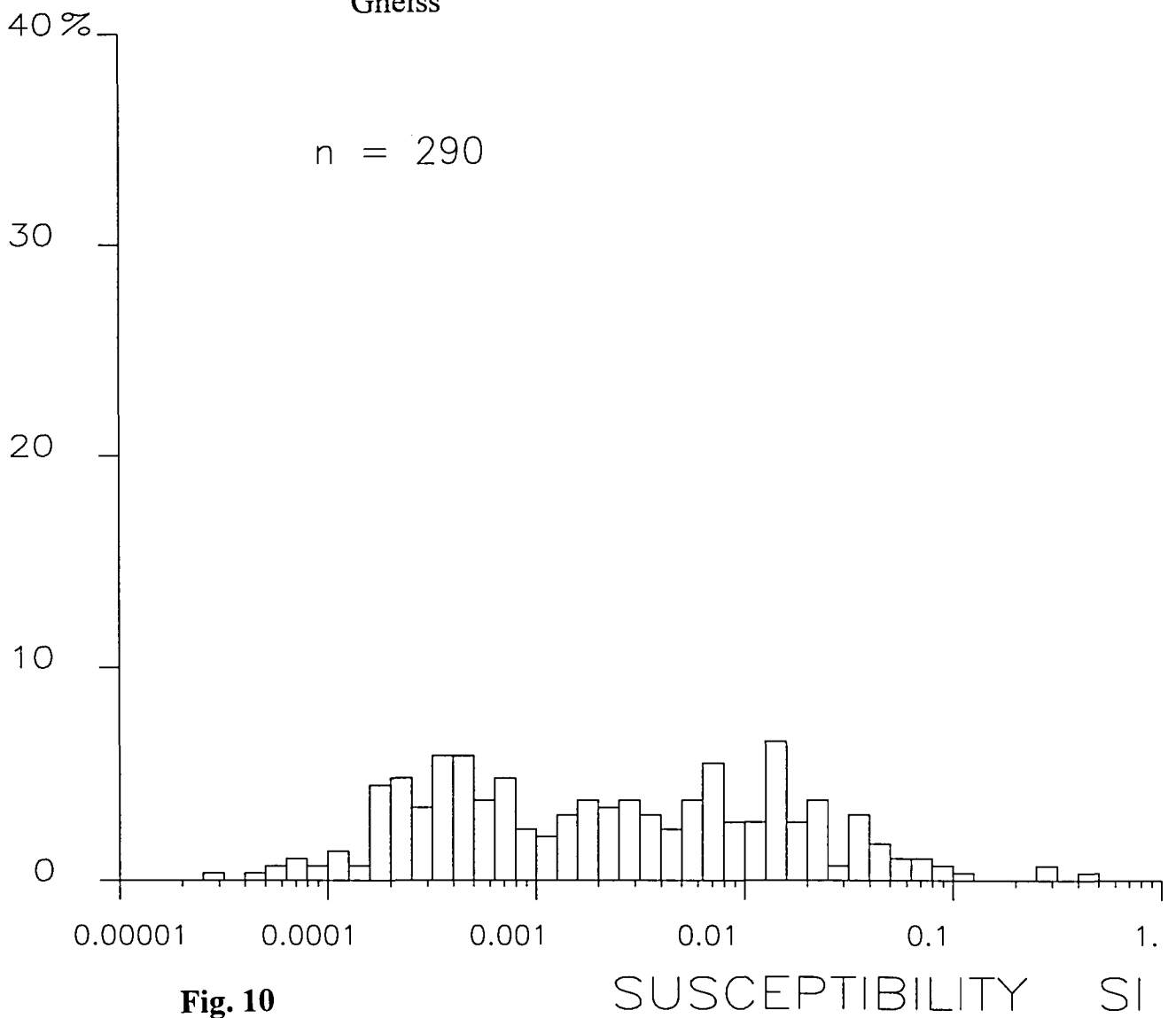


Fig. 10

PRECAMBRIAN ROCKS  
WESTERN GNEISS REGION  
Granodioritic Gneiss

n = 46

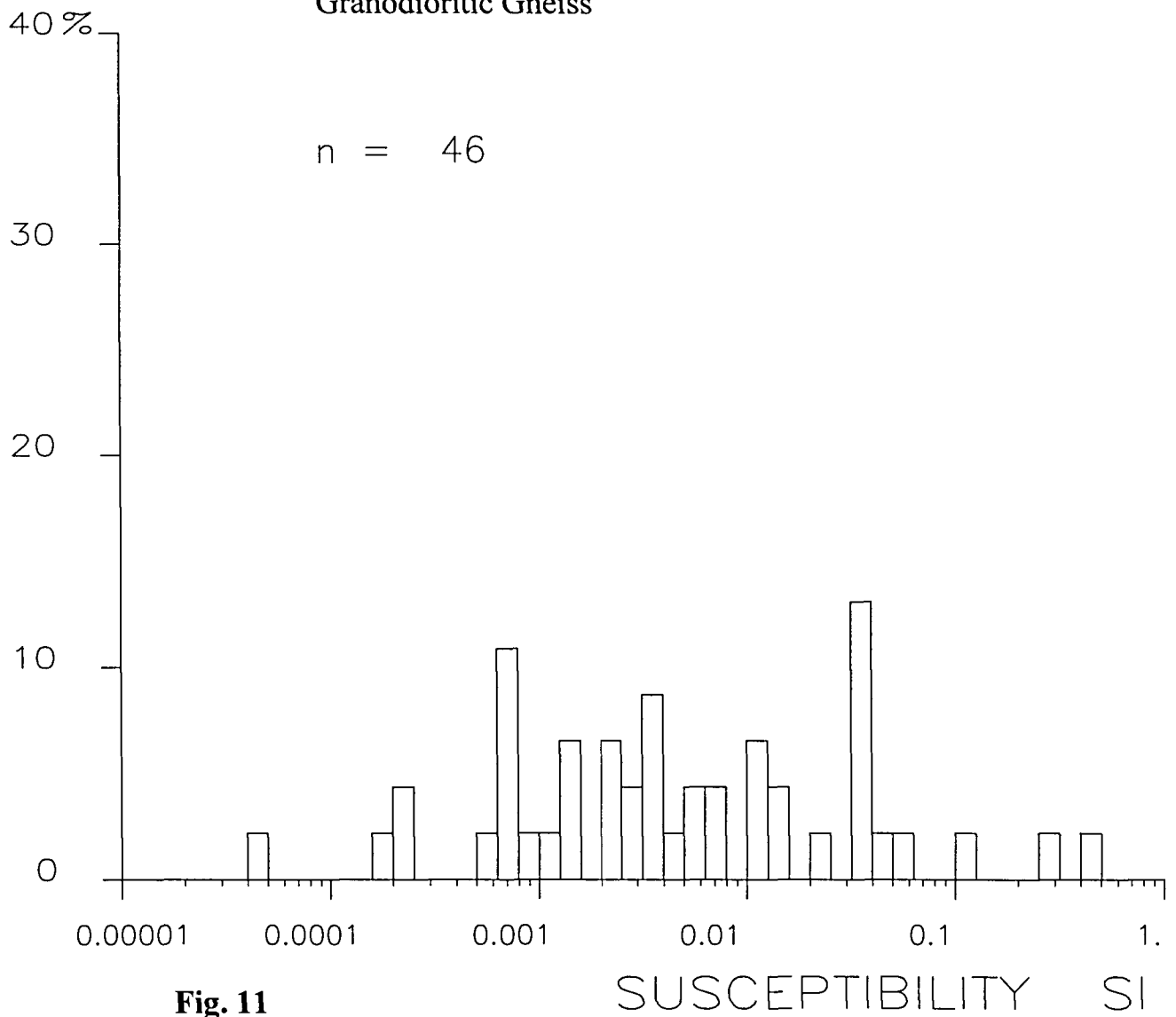


Fig. 11

PRECAMBRIAN ROCKS  
WESTERN GNEISS REGION  
Augen Gneiss

n = 47

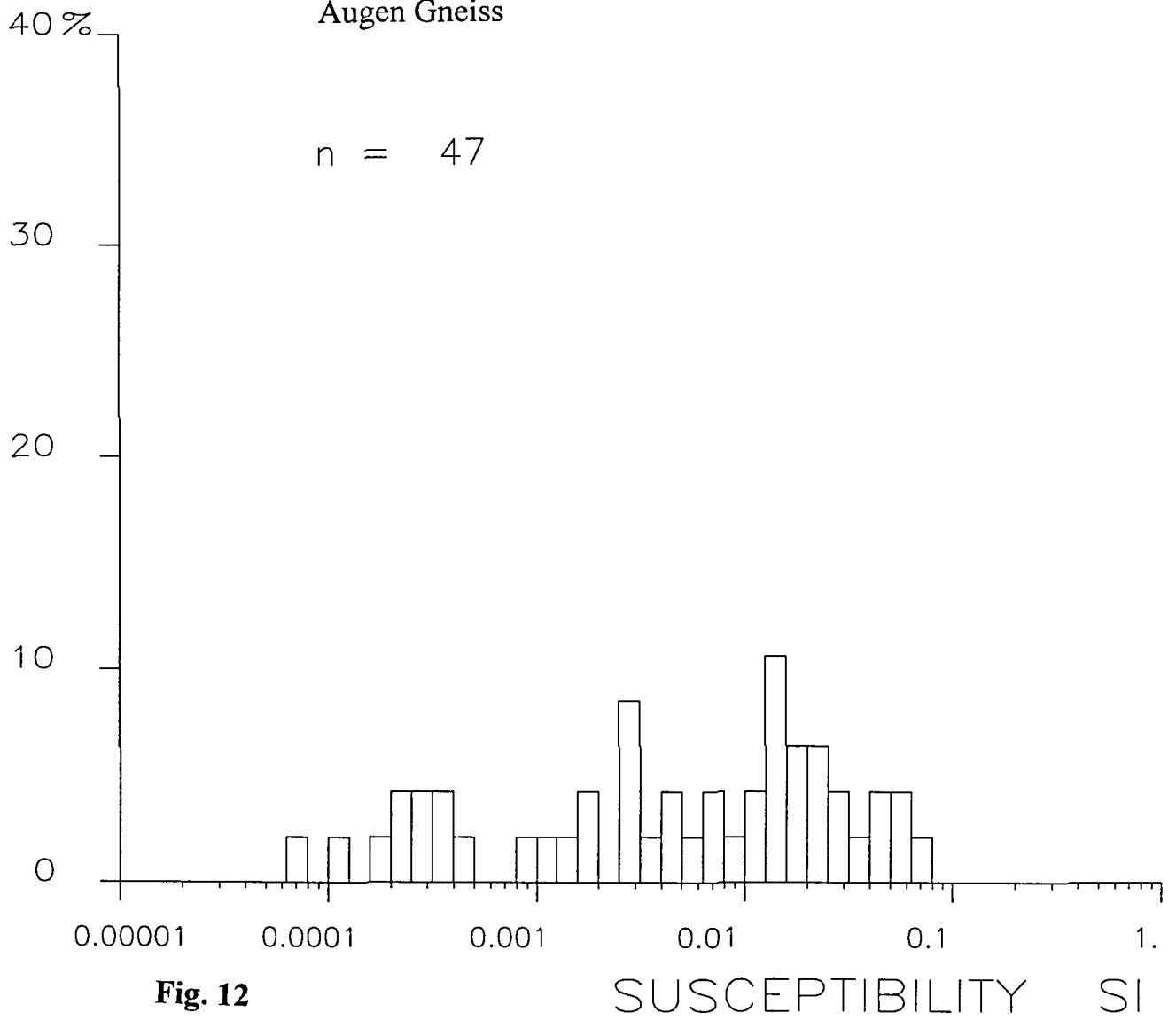


Fig. 12

SUSCEPTIBILITY SI

PRECAMBRIAN ROCKS  
WESTERN GNEISS REGION  
Granitic Gneiss  
n = 34

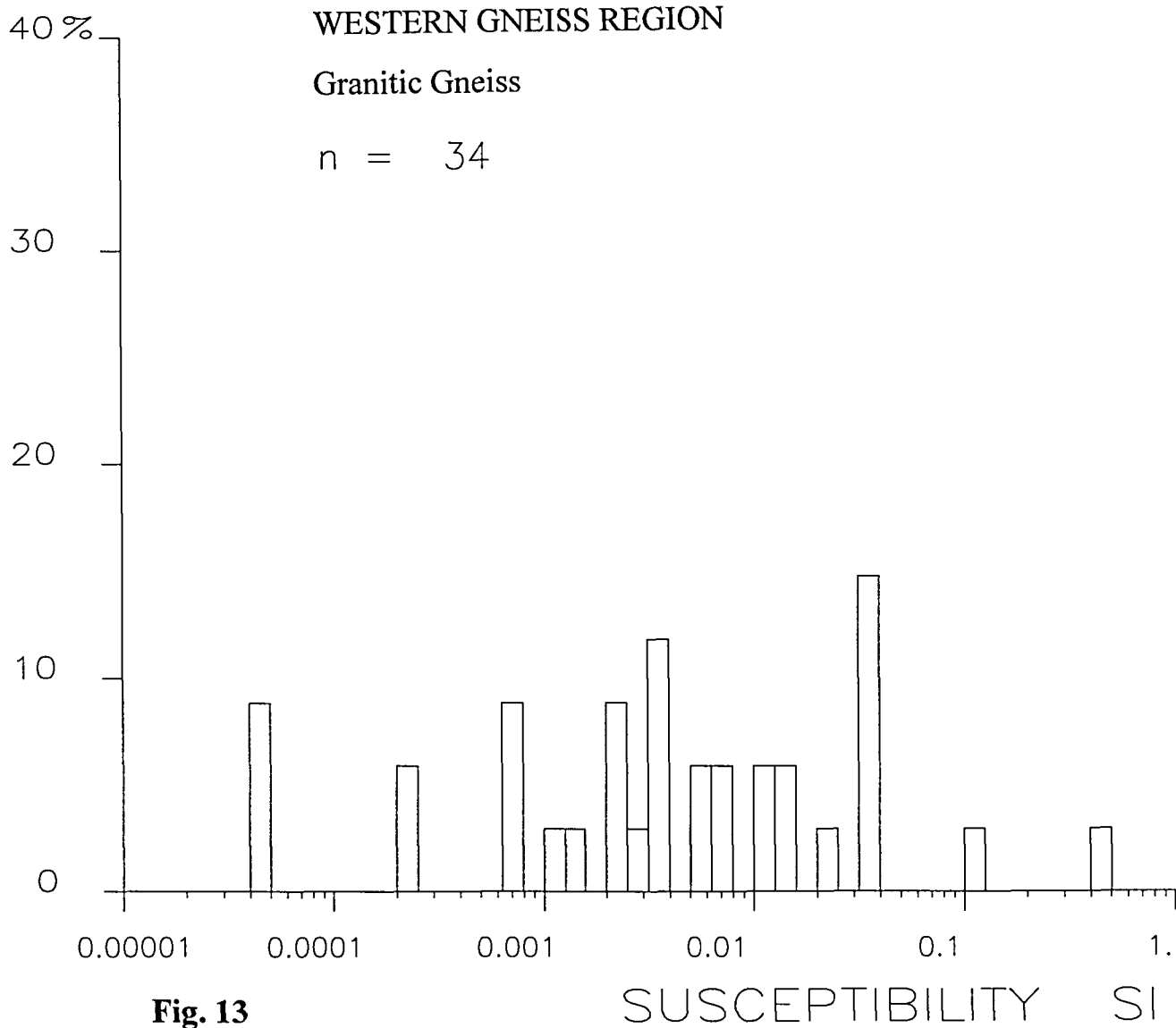


Fig. 13

PRECAMBRIAN ROCKS  
WESTERN GNEISS REGION  
Micagneiss

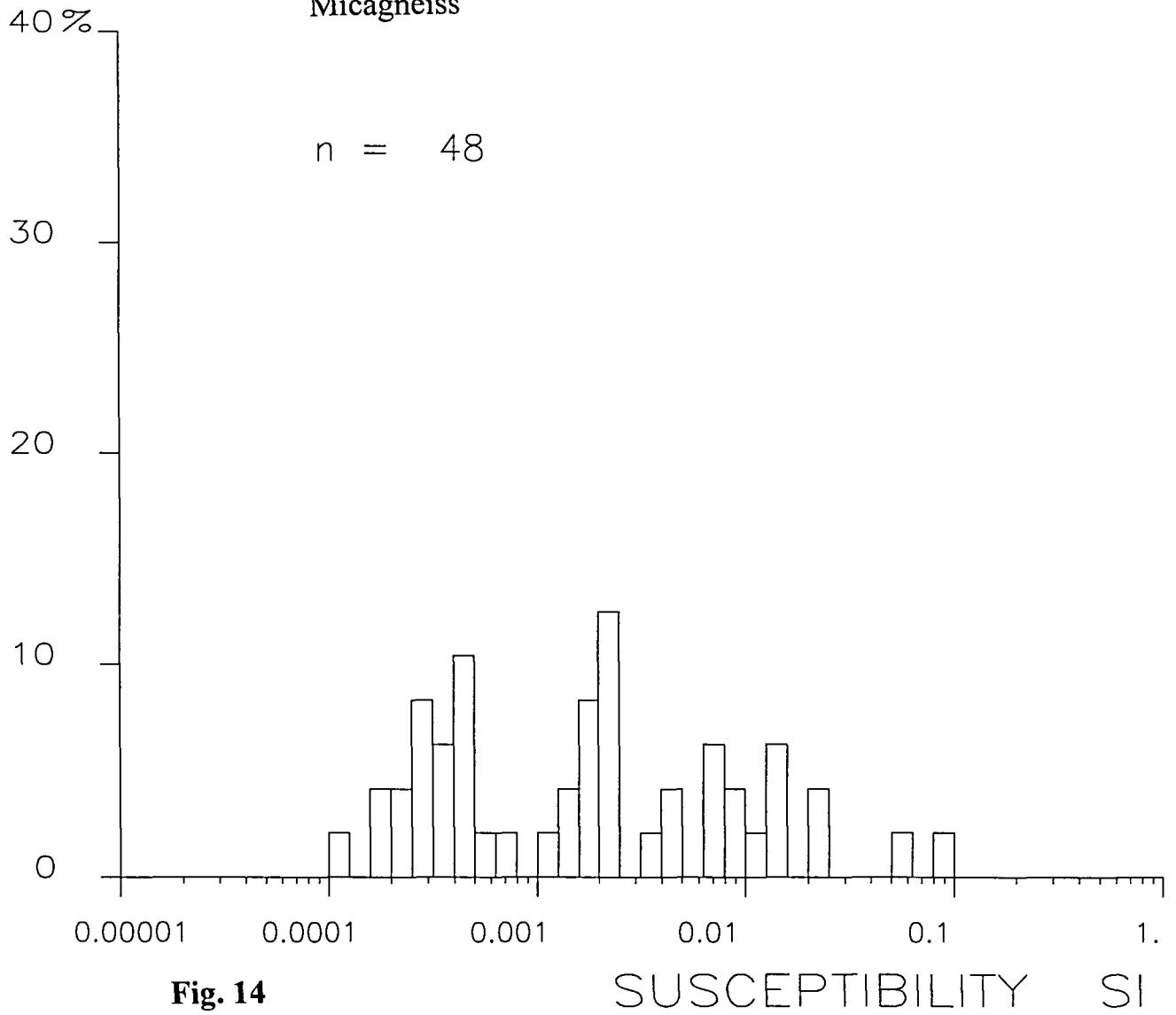


Fig. 14

PRECAMBRIAN ROCKS  
WESTERN GNEISS REGION  
Eclogite

n = 612

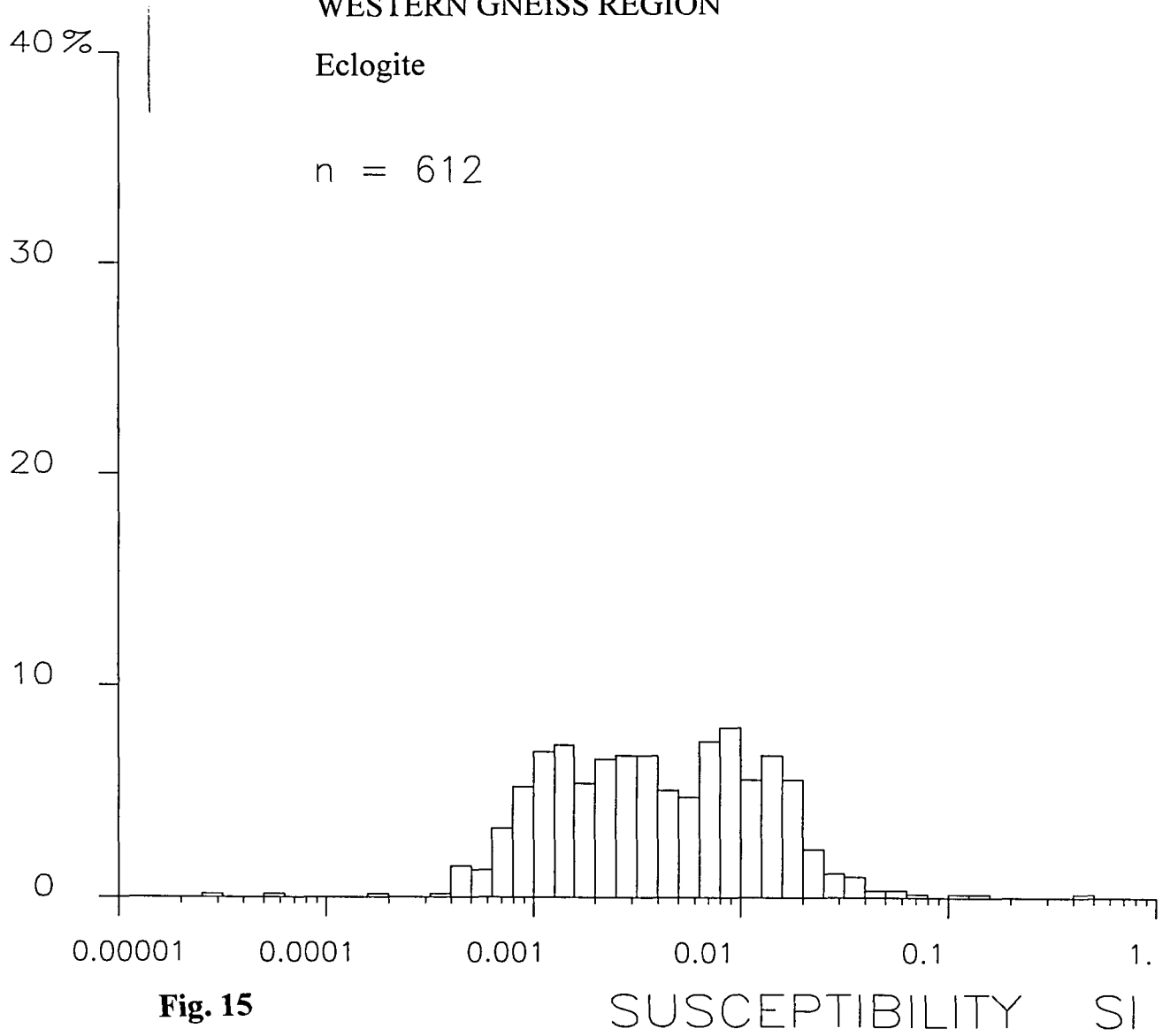


Fig. 15

SUSCEPTIBILITY SI



CALEDONIAN ROCKS

Gneiss, greenschist

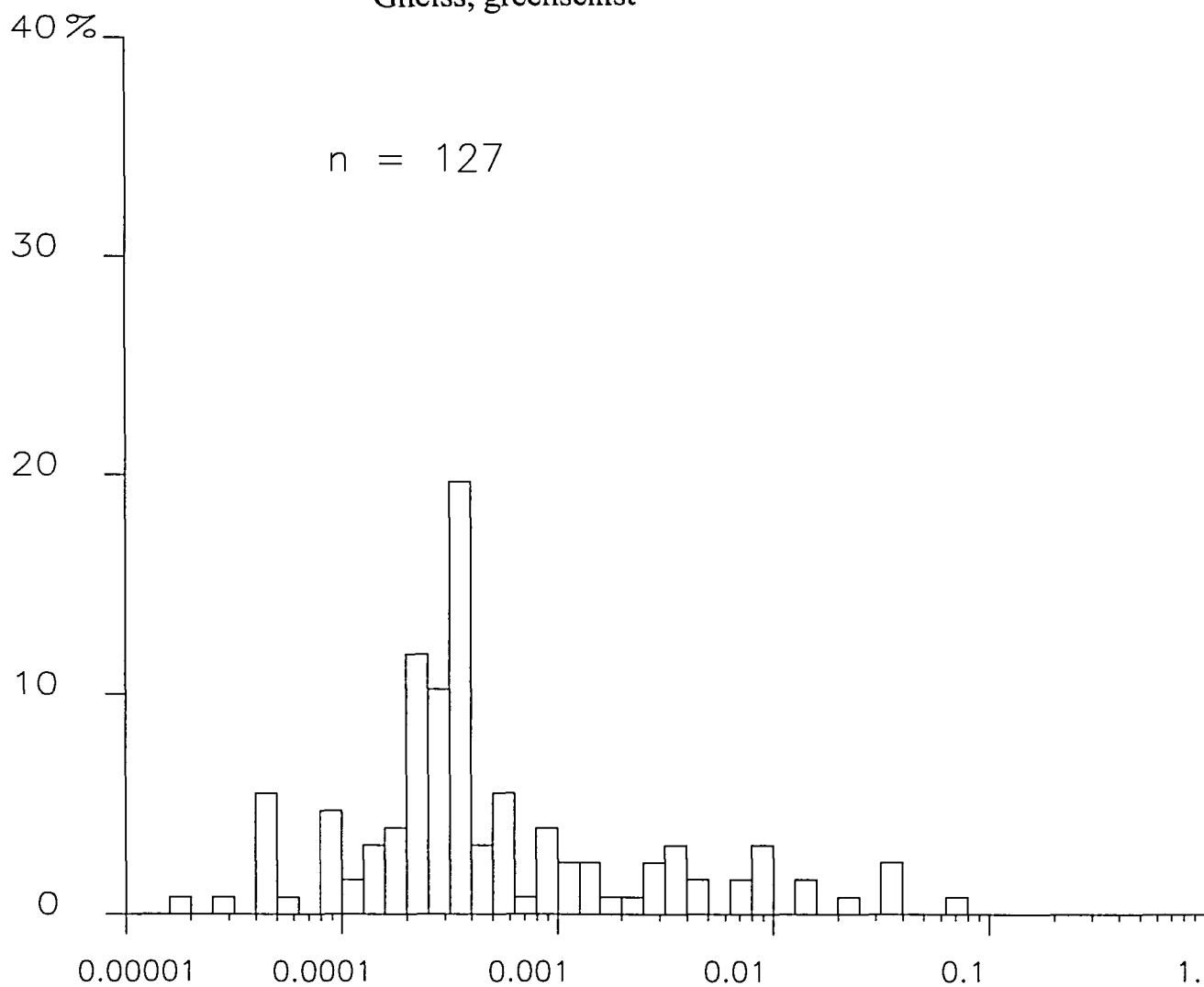


Fig. 16

SUSCEPTIBILITY SI

CALEDONIAN ROCKS

Psammitic rocks, pelitic rocks

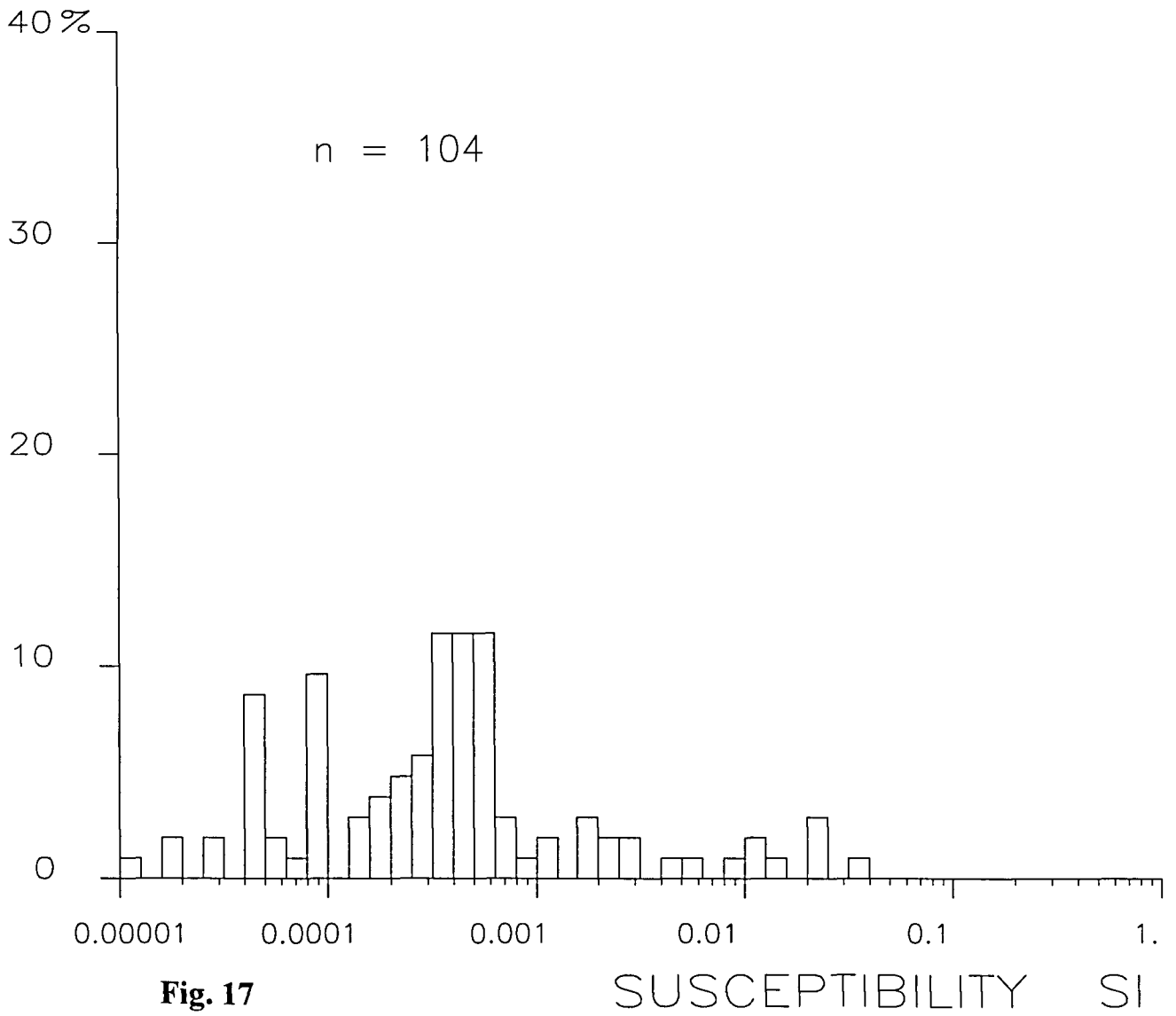
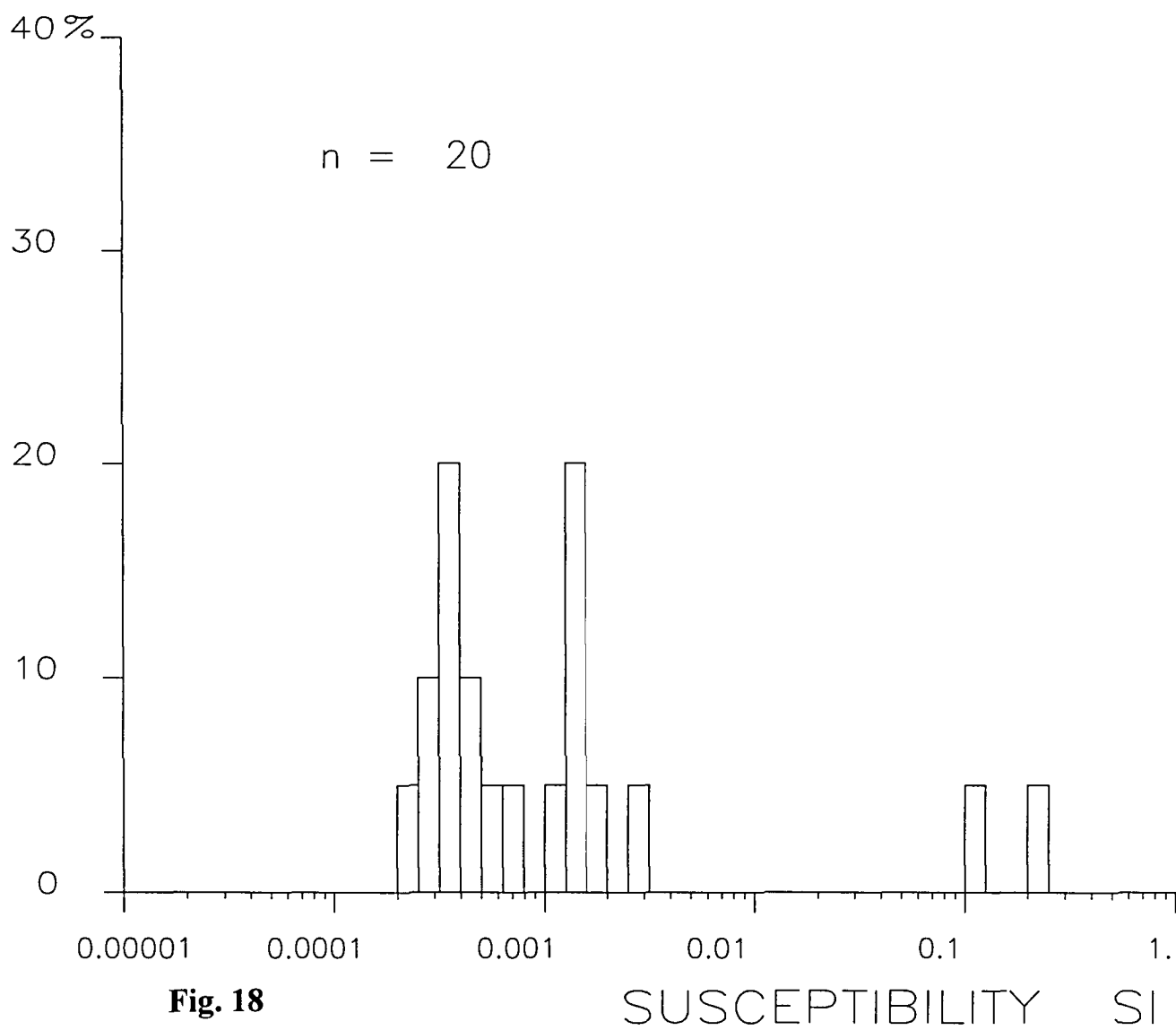


Fig. 17

SUSCEPTIBILITY SI

CALEDONIAN ROCKS

Basic volcanites, greenschist



DEVONIAN SEDIMENTARY ROCKS

Psammitic rocks, pelitic rocks

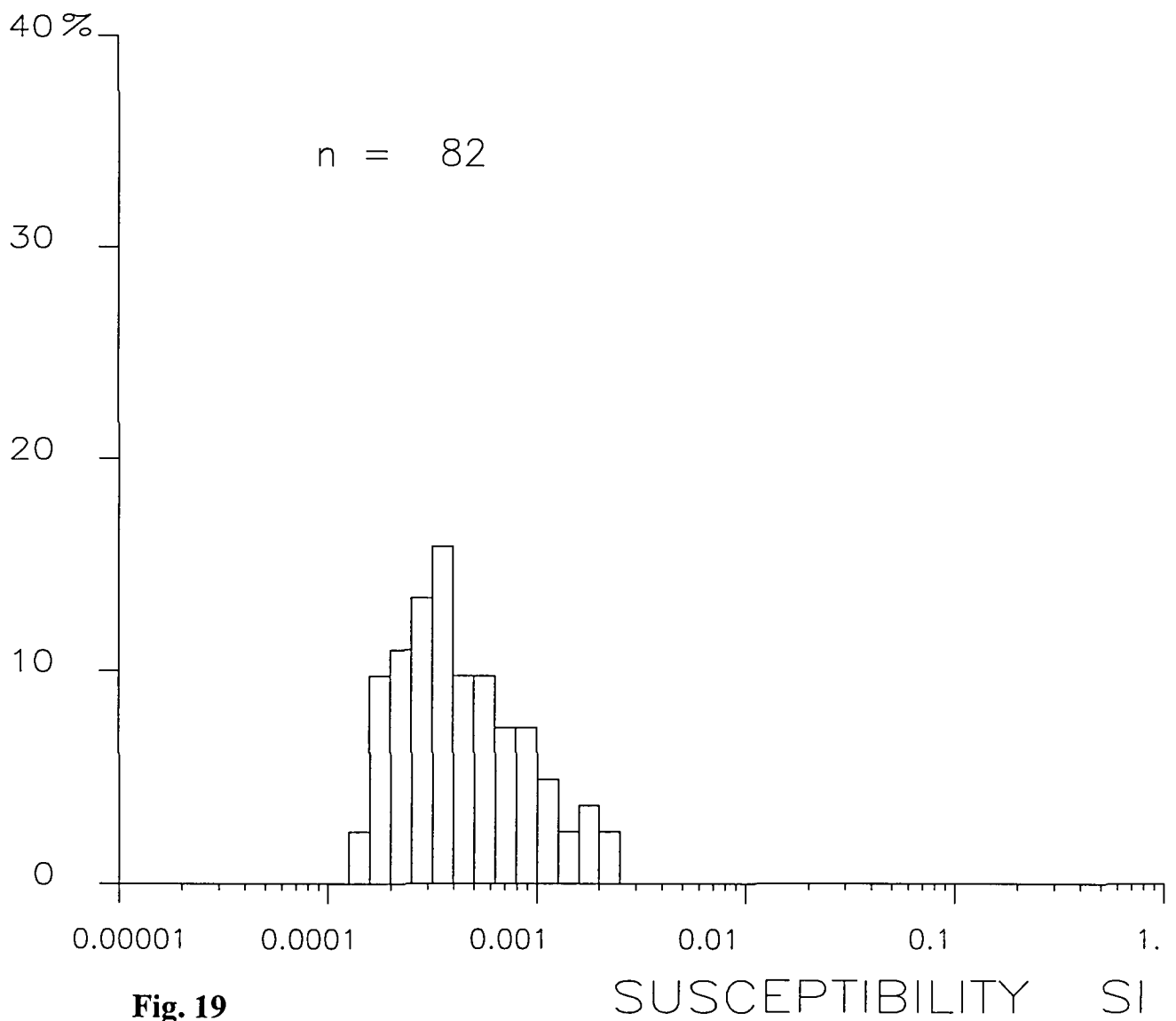


Fig. 19

# NORDVESTLANDET

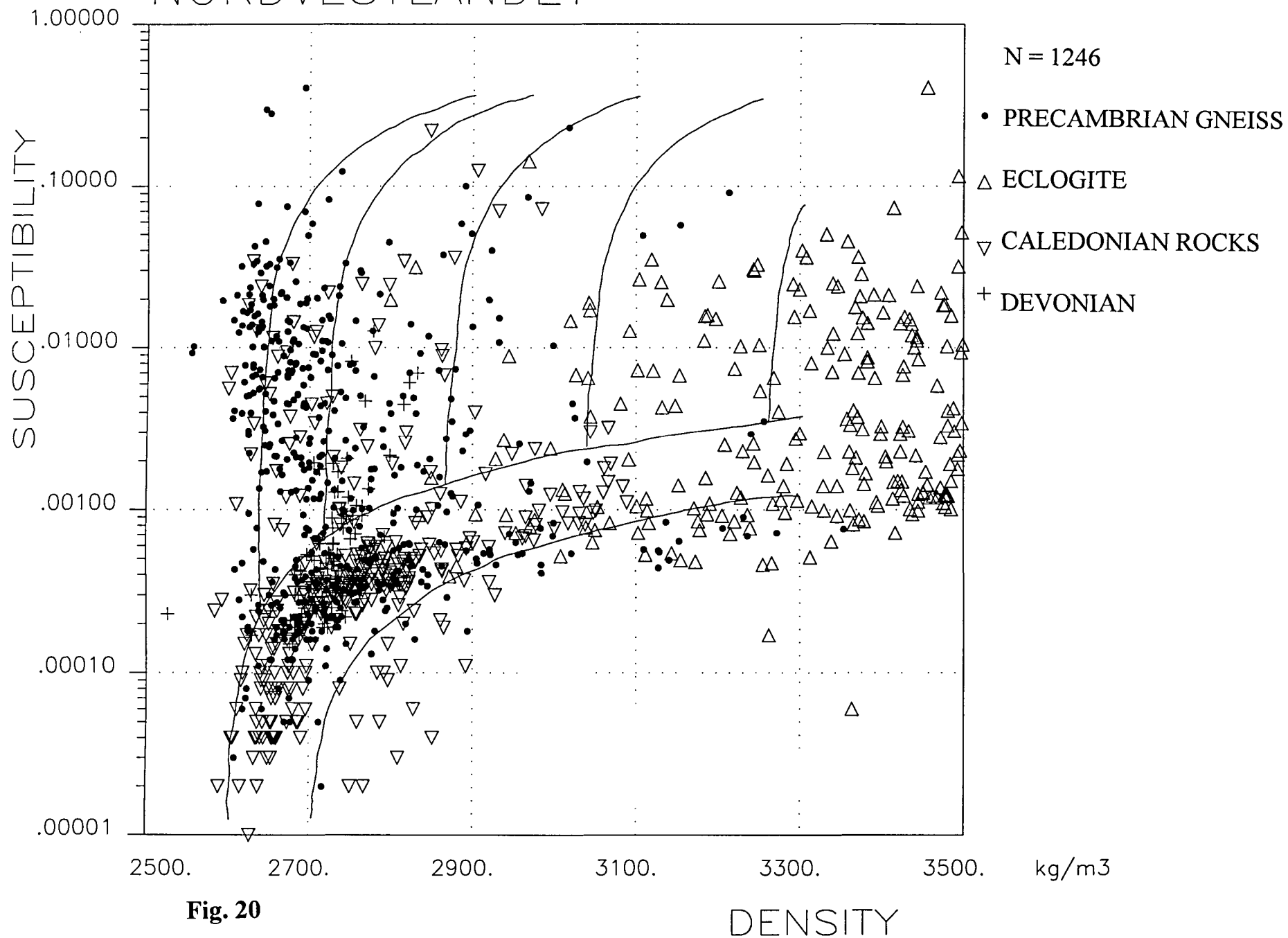
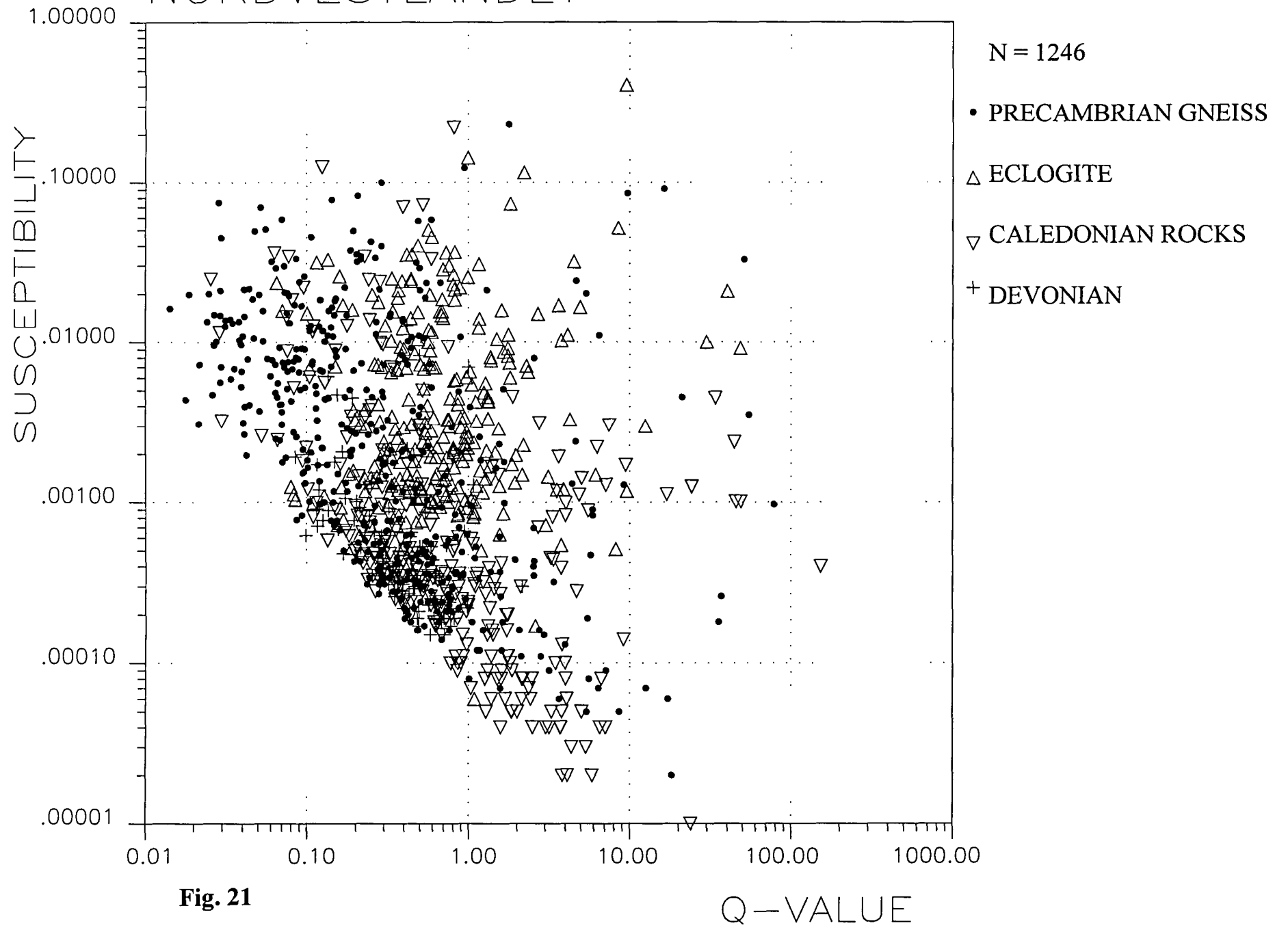


Fig. 20

# NORDVESTLANDET



**Fig. 21**

Q-VALUE